AD-A184 960 CORRELATION OF AIR PRESSURE DROP AND FLAME ARRESTOR CHARACTERISTICS FOR E..(U) DAYTON UNIV OH RESEARCH INST J E MINARDI ET AL. NOV 86 UDR-TR-86-115 1/1

UNCLASSIFIED AFWAL-TR-86-2007 F33615-84-C-2411 F/G 13/12 NL

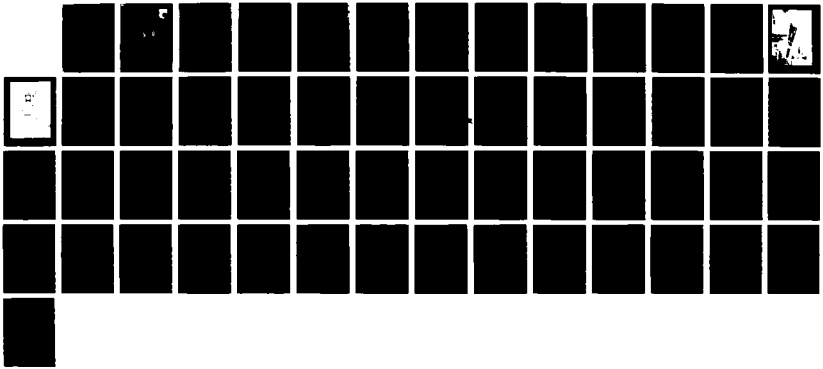

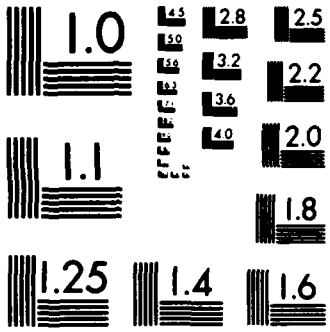

MICROCOPY RESOLUTION TEST CHART
NATIONAL BUREAU OF STANDARDS-1963-A

(2)

AD-A184 960

AFWAL-TR-86-2087

CORRELATION OF AIR PRESSURE DROP AND FLAME ARRESTOR CHARACTERISTICS FOR EXPLOSION SUPPRESSION MATERIALS

John E. Minardi
Maurice O. Lawson

University of Dayton
Research Institute
300 College Park
Dayton, Ohio 45469

November 1986

Final Report for Period February 1985 - January 1986

Approved for public release; distribution is unlimited

AERO PROPULSION LABORATORY
AIR FORCE WRIGHT AERONAUTICAL LABORATORIES
AIR FORCE SYSTEMS COMMAND
WRIGHT-PATTERSON AIR FORCE BASE, OHIO 45433-6563

UNCLASSIFIED

SECURITY CLASSIFICATION OF THIS PAGE

REPORT DOCUMENTATION PAGE

1a. REPORT SECURITY CLASSIFICATION Unclassified	1b. RESTRICTIVE MARKINGS
2a. SECURITY CLASSIFICATION AUTHORITY 2b. DECLASSIFICATION/DOWNGRADING SCHEDULE	3. DISTRIBUTION/AVAILABILITY OF REPORT Approved for public release; distribution is unlimited
4. PERFORMING ORGANIZATION REPORT NUMBER(S) UDR-TR-86-115	5. MONITORING ORGANIZATION REPORT NUMBER(S) AFWAL-TR-86-2087
6a. NAME OF PERFORMING ORGANIZATION University of Dayton Research Institute 6b. OFFICE SYMBOL (If applicable)	7a. NAME OF MONITORING ORGANIZATION Aero Propulsion Laboratory (POSH/POS) Air Force Wright Aeronautical Laboratories
6c. ADDRESS (City, State and ZIP Code) 300 College Park Dayton, Ohio 45469	7b. ADDRESS (City, State and ZIP Code) Air Force Systems Command Wright-Patterson Air Force Base, Ohio 45433-6563
8a. NAME OF FUNDING/SPONSORING ORGANIZATION Aero Propulsion Laboratory 8b. OFFICE SYMBOL (If applicable) AFWAL/POSH	9. PROCUREMENT INSTRUMENT IDENTIFICATION NUMBER F33615-84-C-2411 (Task XII)
8c. ADDRESS (City, State and ZIP Code) Aero Propulsion Laboratory (AFWAL/POSH) Air Force Wright Aeronautical Labs (AFSC) Wright-Patterson Air Force Base OH 45433-6563	10. SOURCE OF FUNDING NOS. PROGRAM ELEMENT NO.: 62203F PROJECT NO.: 3048 TASK NO.: 07 WORK UNIT NO.: 87
11. TITLE (Include Security Classification) Correlation of Air Pressure (cont'd back)	
12. PERSONAL AUTHOR(S) Minardi, John E. and Lawson, Maurice O.	
13a. TYPE OF REPORT Final 13b. TIME COVERED FROM 850201 TO 860131	14. DATE OF REPORT (Yr., Mo., Day) November 1986 15. PAGE COUNT 55
16. SUPPLEMENTARY NOTATION	

17. COSATI CODES			18. SUBJECT TERMS (Continue on reverse if necessary and identify by block number)
FIELD	GROUP	SUB. GR.	Flame arresting, Explosion suppression, Fire Protecting foam, Polyurethane foam, Explosion Suppressant foam, Quenching diameter
21	02		
21	04		

19. ABSTRACT (Continue on reverse if necessary and identify by block number)

In this report a theory is presented for predicting the pressure rise versus void fraction in the flame tube located at Wright-Patterson Air Force Base. The effects of initial temperature and pressure are included in the theory. A study of the heat losses in the flame tube is presented and an empirical fit to the cool down phase of the pressure time history data is developed. An equation for correlating the friction factors measured in the pressure drop rig with the hydraulic diameter of the foam is developed. An equation for the critical hydraulic diameter (or "quenching diameter") as a function of initial pressure and temperature is also given in the report. The theoretical results are compared to experimental data and are shown to compare favorably.

20. DISTRIBUTION/AVAILABILITY OF ABSTRACT UNCLASSIFIED/UNLIMITED ☒ SAME AS RPT ☐ DTIC USERS ☐	21. ABSTRACT SECURITY CLASSIFICATION Unclassified
22a. NAME OF RESPONSIBLE INDIVIDUAL Lynne M. Schoen	22b. TELEPHONE NUMBER (Include Area Code) (513) 255-3100 22c. OFFICE SYMBOL AFWAL/POSH

DD FORM 1473, 83 APR EDITION OF 1 JAN 73 IS OBSOLETE.

UNCLASSIFIED

SECURITY CLASSIFICATION OF THIS PAGE

Block 11 (continued)

Drop and Flame Arrestor Characteristics for Explosion Suppression Materials

FOREWORD

This report was prepared by the Aerodynamics and Energy Conversion Group of the Aerospace Mechanics Division, University of Dayton Research Institute, Dayton, Ohio. The work was funded by the Air Force Wright Aeronautical Laboratories, Aero Propulsion Laboratory, Fire Protection Branch (AFWAL/POSH) and Fuels and Lubrication Division (AFWAL/POS) under Contract F33615-84-C-2411, Task XII. The task monitor was Lynne Schoen.

The authors wish to express appreciation to Ms. Schoen for her valuable assistance and comments during this work. The authors also wish to thank our students Mr. Jim deVries, Mr. Dave Geis, and Mr. Tom Prevish for their assistance during this program. A special thanks is due to Ms. Carolyn Gran for typing this report and its many complex equations.

TABLE OF CONTENTS

LIST OF ILLUSTRATIONS

LIST OF ILLUSTRATIONS (Concluded)

LIST OF SYMBOLS

A_s = surface area of foam

A_t = cross sectional area

C = constant

C_{iR} = circumference

C_p = specific heat at constant pressure

C_v = specific heat at constant volume

D_h = hydraulic diameter

D_h^* = critical value of hydraulic diameter

D_{ho}^* = critical value of hydraulic diameter at 1 atmosphere and 80°F

f = friction factor per inch of foam

f_{COR} = friction factor per inch of foam corrected to the standard conditions

f_{TOT} = total friction factor for the foam thickness

g = acceleration due to gravity

H = heat of reaction

h_{fc}^* = heat transfer coefficient in free convection

h_i^* = initial value of heat transfer coefficient

h_p^* = heat transfer coefficient of the products

h_u^* = heat transfer coefficient of the unburnt reactants

K = function of the vapor pressure and L_b

L = length of flame tube

L_b = beam length in meters

L_c = length of void region

L_p = length of products region

L_r = length of relief volume region

L_u = length of region containing the unburnt reactants

m = mass or an exponent

m_e = an exponent

$\dot{m}_f$ = mass flow rate through the foam

$\dot{m}_{fi}$ = initial value of mass flow rate through the foam

m_p = mass of products

m_r = mass of gas in the relief volume

m_u = mass of unburnt reactants

m_{uo} = initial value of mass of unburnt reactants

N_{Pe} = Peclet number = $D_h V_\ell / \alpha$

P = pressure

P_c = vapor pressure of carbon dioxide

P_i = initial pressure at the start of the cool down phase

P_o = initial pressure in the flame tube before combustion

P_{pi} = number of pores per inch

P_R = pressure in relief volume

P_w = vapor pressure of water

Q = heat transfer

$\dot{Q}_T$ = total heat transfer rate

$\dot{Q}_u$ = heat transfer rate from the unburnt region

S = specific surface area of the foam, ft^2/ft^3

t = time

t_p = time of the peak

T_f = adiabatic flame temperature

T_p = temperature of the products

T_u = temperature of the unburnt reactants

T_w = initial temperature equal to the wall temperature

v = specific volume

v_o = initial specific volume

v_u = specific volume of the unburnt reactants

V = total volume

V_f = flame speed

V_{fo} = initial flame speed

V_ℓ = laminar flame speed

V_p = total volume of products

V_u = total volume of unburnt reactants

α = thermal diffusivity

β = coefficient of expansion (1/T for an ideal gas)

γ = ratio of the specific heats

ε = emissivity

ρ = density

ρ_o = initial density

ρ_u = denisty of the unburnt reactants

ρ_{uo} = initial density of the unburnt reactants

κ = thermal conductivity

μ = viscosity

INTRODUCTION

In order to reduce the emphasis which is placed on flame arresting tests, another reliable method for characterizing explosion suppressants was needed. Therefore, this study was undertaken to establish if a correlation could be developed between the air pressure drop characteristics and flame arrestor characteristics for explosion suppression materials. A reliable test procedure was developed for measuring air pressure drop across a foam sample in the pressure drop rig and is presented in Reference 1. The pressure drop rig is shown in Figure 1.

The flame tube rig is shown in Figure 2. The flame tube test chamber consists of a rectangular stainless steel tank capable of containing combustion overpressures as high as 120 psig. The test section is square (1 ft by 1 ft) and is 7.5 ft long.

In qualifying a foam, tests are run in accordance with Military Specification MIL-B-83054B (USAF) in the flame tube using a propane-air mixture at initial pressures of 14.7 and 17.7 psia. Examples of these qualifying runs are given in Reference 2.

Two types of tests are run in the flame tube: flame arrestor tests and explosion suppression tests. Currently a fine pore (small hole) foam is identified as a flame arrestor and the coarse pore (large hole) foam is a combustion overpressure suppressor. Both types of foam will suppress a combustion overpressure but the fine pore foam will arrest the flame while the coarse pore foam may let the flame pass through.

In order to develop a correlation between the pressure drop tests, the results of which can be related to foam pore size, and the flame tube tests, the results of which are also related to foam pore size through increased heat transfer, a theory for the pressure rise in the flame tube was developed which includes heat loss.

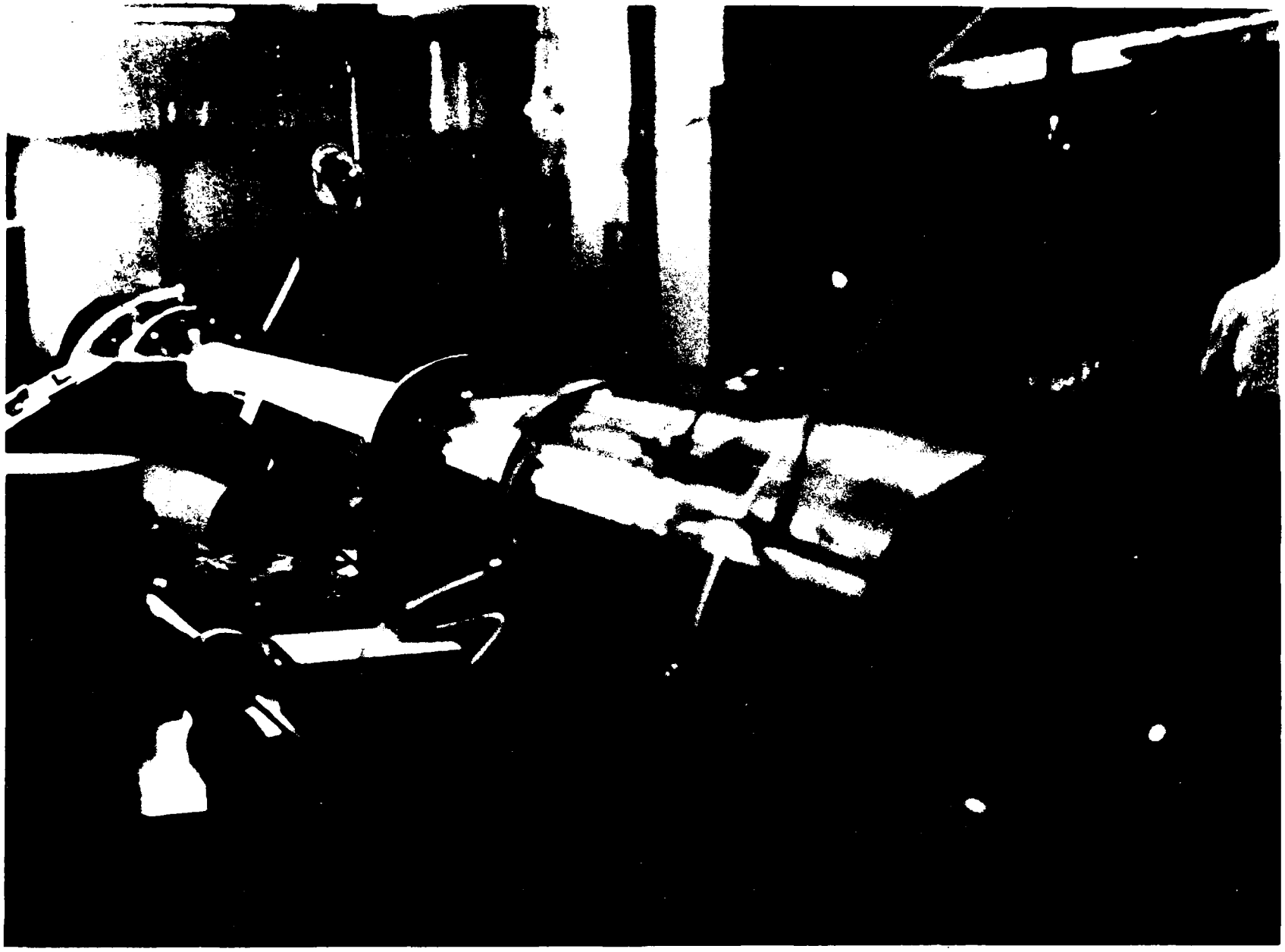

Figure 1. Photograph of the pressure drop rig located at Wright-Patterson Air Force Base.

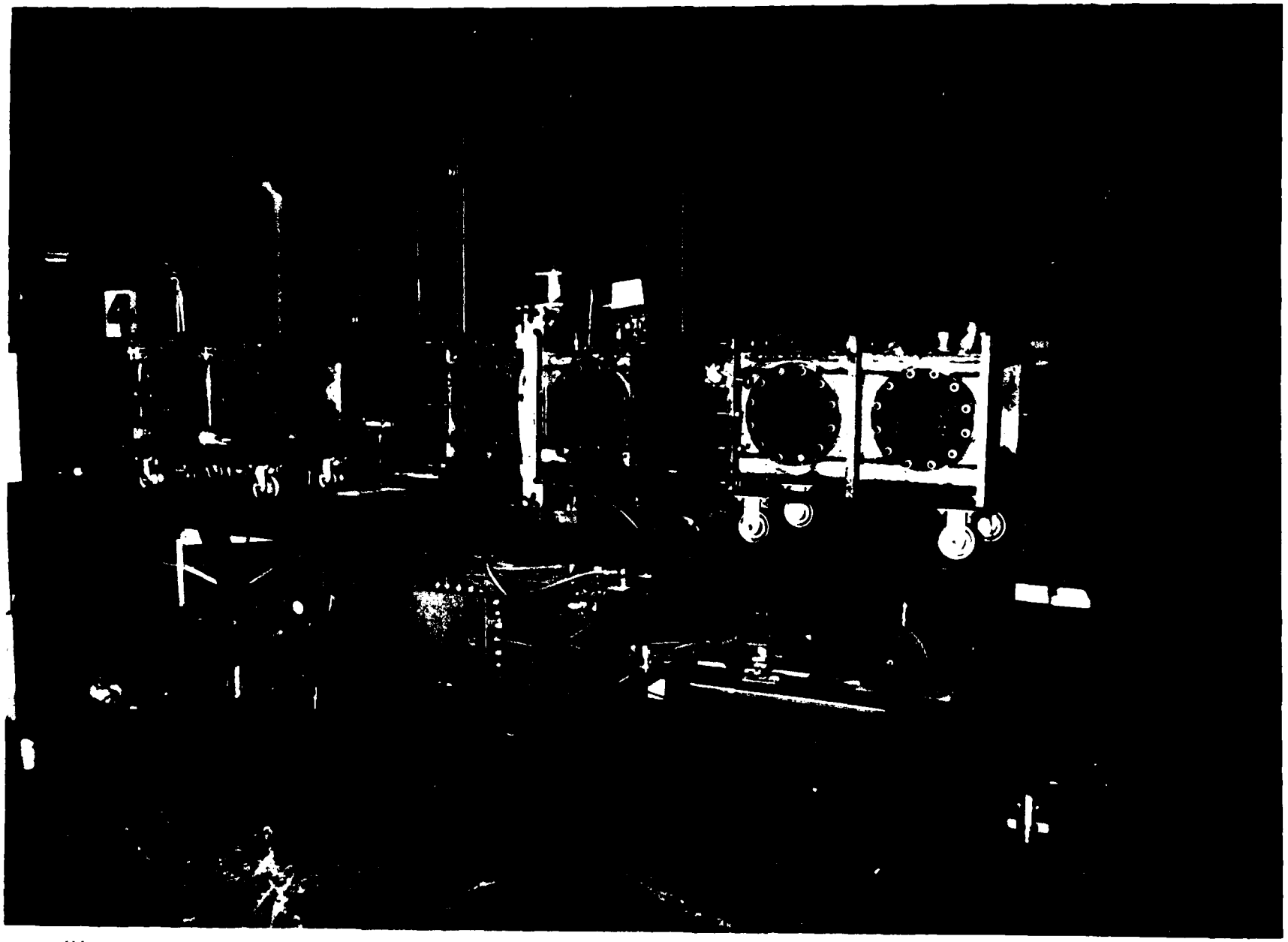

Figure 5. Photograph of the flame tube located at Wright-Patterson Air Force Base.

Since it has been established that the performance of arrestors are essentially independent of the material properties of the arrestor and only depend on cell dimensions (see Reference 3), it was concluded that the theory could be developed independent of the material from which the flame arrestor is made. The theory does depend on the fuel-air mixture and the initial temperature and pressure. In the next section the pressure rise theory is developed for the flame tube.

PRESSURE RISE THEORY

The initial form of the theory was developed to closely match the pressure rise that occurs in the flame tube when a mixture of propane and air is burnt without a flame arrestor material present. Figure 3 shows a schematic of the flame tube showing the two regions on either side of the flame: the products of combustion on the left and the unburnt reactants on the right. The following simplifying assumptions are made:

1. The gas is uniformly mixed in each region.
2. The pressure is constant throughout the tube at any instant (i.e., the speed of sound is much faster than the flame speed, V_f).
3. The reactants are compressed in a reversible process.
4. The number of moles of products is approximately equal to the number of moles of reactants.
5. Ideal gas equations are valid for both regions.
6. The specific heats of the reactants and products are approximately equal.
7. The initial temperature of the gas is equal to the wall temperature.
8. The wall temperature remains constant.

The conservation of mass for the two regions of Figure 3 is

$$m_P + m_u = m \tag{1}$$

Since the volume is also constant, we have for the two regions

$$V_P + V_u = V \tag{2}$$

Using the specific volumes in Equation (2) and combining it with Equation (1) yields after rearrangement

$$v_u m_P\left(\frac{v_P}{v_u} - 1\right) = m v_u\left(\frac{v_o}{v_u} - 1\right) \tag{3}$$

Since the pressure in both regions is the same and the number of moles are assumed to be equal then it follows from the ideal gas equation that

$$\frac{v_P}{v_u} = \frac{T_P}{T_u} \tag{4}$$

In view of Equations (3) and (4) it follows that

$$\frac{m_P}{m}\left(\frac{T_P}{T_u} - 1\right) = \frac{v_o}{v_u} - 1 \tag{5}$$

The energy equation, including the heat released by the reaction, is

$$m_P C_v(T_P - T_w) - m_P H + m_u C_v(T_u - T_w) = Q \tag{6}$$

We have assumed that the specific heats of the unburnt reactants and the products are the same. The value of H in Equation (6) is related to the adiabatic flame temperature, T_f, by the following

$$H = C_v(T_f - T_w) \tag{7}$$

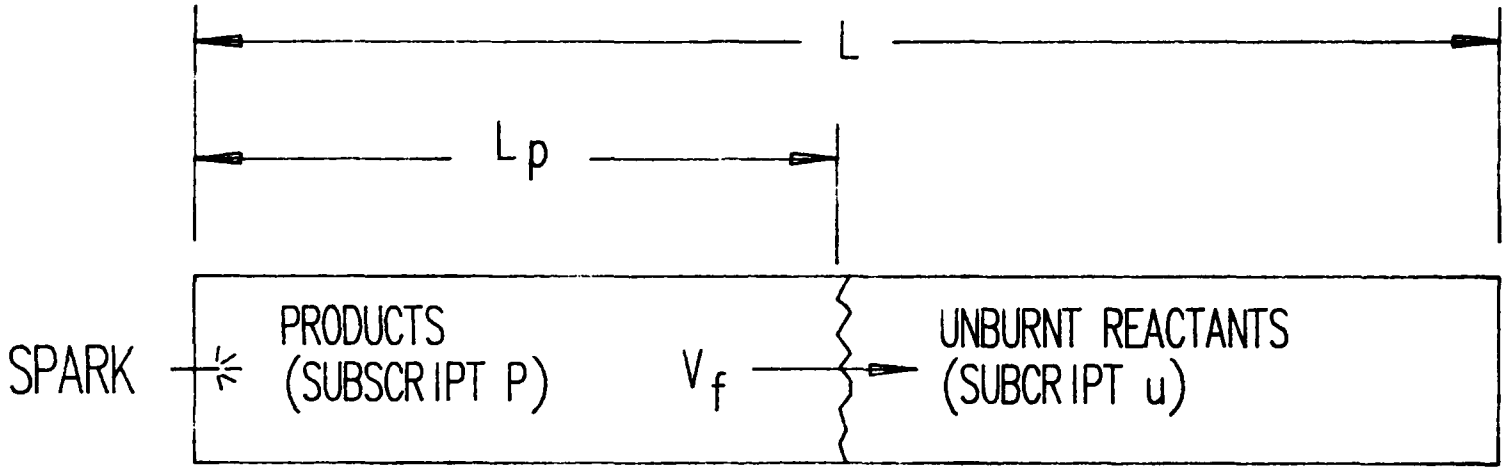

Figure 3. Schematic of the flame tube showing the two regions on either side of the flame.

Substituting Equations (7) and (1) into (6) and rearranging yields

$$\frac{m_P}{m}\frac{T_u}{T_w}\left(\frac{T_P}{T_u} - 1\right) = \frac{m_P}{m}\frac{(T_f - T_w)}{T_w} + 1 - \frac{T_u}{T_w} + \frac{Q}{C_v m T_w} \tag{8}$$

In view of Equation (5) above

$$\frac{T_u}{T_w}\frac{v_o}{v_u} = \frac{m_P}{m}\frac{(T_f - T_w)}{T_w} + 1 + \frac{Q}{C_v m T_w} \tag{9}$$

but from the ideal gas equation

$$\frac{P}{P_o} = \frac{T_u}{v_u} \cdot \frac{v_o}{T_w} \tag{10}$$

Hence, it follows from Equations (9) and (10) that

$$\frac{P}{P_o} = \frac{m_P}{m}\left(\frac{T_f - T_w}{T_w}\right) + 1 + \frac{Q}{C_v m T_w} \tag{11}$$

The rate of product production is related to the flame speed V_f as

$$\frac{dm_P}{dt} = V_f \rho_u A_t \tag{12}$$

According to Reference 4, the laminar flame speed is independent of pressure for second-order reactions which occur for many hydrocarbon fuels. However, the flame speed is a function of the temperature, T_u, in the unburned reactants. According to Reference 4, the flame speed is given by

$$V_f = V_{fo}\left(\frac{T_u}{T_w}\right)^{m_e} \tag{13}$$

where the exponent m_e ranges between 1.5 and 2. Although the turbulent flame speed is much greater than the laminar flame

speed, we will assume that the variation with the temperature is the same as given by Equation (13) and the initial value of the speed, V_{fo}, will be a parameter for fitting the data.

Using the ideal gas equation and Equation (13) with Equation (12) yields

$$\frac{d}{dt}\left(\frac{mP}{m}\right) = \frac{V_{fo}}{L}\,\frac{P}{P_o}\left(\frac{T_u}{T_w}\right)^{m_e - 1} \tag{14}$$

If we assume that the reactants are compressed reversibly, then we have

$$\dot{Q}_u/m_u = C_P\,\frac{dT_u}{dt} - v\,dP/dt \tag{15}$$

which results in

$$\frac{d\left(\frac{T_u}{T_w}\right)}{dt} = \frac{\gamma - 1}{\gamma}\,\frac{T_u}{T_w}\,\frac{P_o}{P}\,\frac{d\left(\frac{P}{P_o}\right)}{dt} + \frac{\dot{Q}_u}{C_P T_w m_R} \tag{16}$$

If the heat transfer is zero in Equations (16) and (11), then an analytic solution can be obtained. Equation (16) results in the well known isentropic relation for an ideal gas:

$$\frac{T_u}{T_w} = \left(\frac{P}{P_o}\right)^{\frac{\gamma - 1}{\gamma}} \tag{17}$$

which can be substituted into Equation (14) with the result

$$\frac{d\left(\frac{mP}{m}\right)}{dt} = \frac{V_{fo}}{L}\left(\frac{P}{P_o}\right)^{\frac{\gamma - 1}{\gamma}\,m_e + \frac{1}{\gamma}} \tag{18}$$

In view of Equation (11) for zero heat transfer we have

$$\frac{d\left(\frac{P}{P_o}\right)}{dt} = \frac{T_f - T_w}{T_w} \frac{d\left(\frac{m_P}{m}\right)}{dt} \tag{19}$$

If we substitute Equation (18) into (19) and integrate the resultant equation the solution is

$$\frac{P}{P_o} = \left[1 + \frac{(1 - m_e)(\gamma - 1)}{\gamma}\left(\frac{T_f}{T_w} - 1\right)\frac{V_{fo}t}{L}\right]^{\frac{\gamma}{(1 - m_e)(\gamma - 1)}} \tag{20}$$

Equation (11), for zero heat transfer, can be used to solve for the mass of products

$$\frac{m_P}{m} = \frac{P/P_o - 1}{T_f/T_w - 1} \tag{21}$$

Equation (21) shows that if $m_P/m = 1$, then $P/P_o = T_f/T_w$ which it should in an adiabatic constant volume burning of the fuel. Since the unburnt reactants are compressed isentropically it follows that

$$\frac{v_o}{v_u} = \left(\frac{P}{P_o}\right)^{1/\gamma} \tag{22}$$

In view of Equation (5) we have

$$\frac{T_P}{T_u} = 1 + \frac{v_o/v_u - 1}{m_P/m} \tag{23}$$

Equations (20) to (23) along with Equation (17) give a complete solution of the rise time histories of all the variables. The equations were used to fit the data shown in Figure 4.

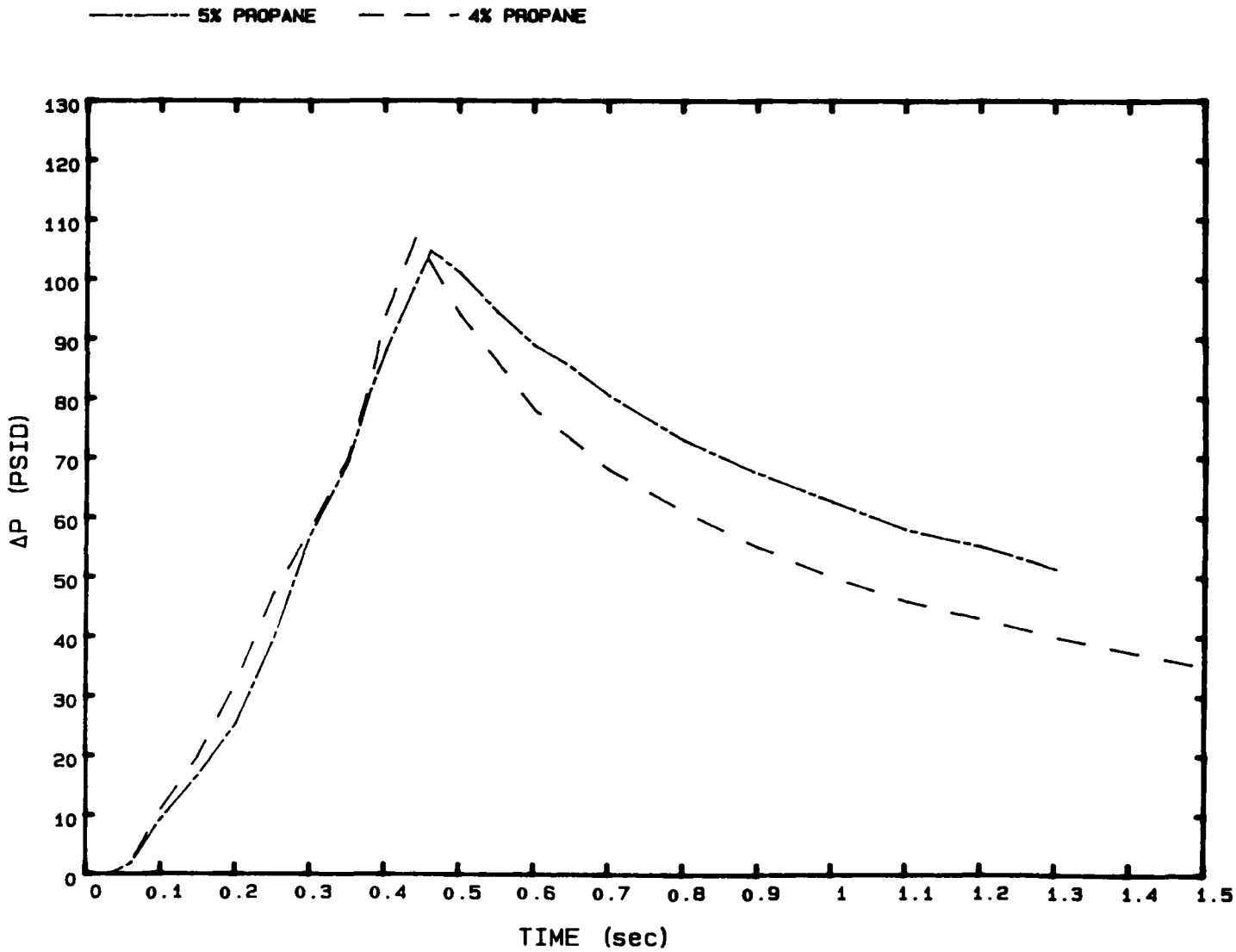

Figure 4. Overpressure versus time in the flame tube without foam.

The curve marked "1" in Figure 4 was plotted from data obtained in a test conducted during the current program. The curve marked "2" in Figure 4 was plotted from data presented in Reference 5. The higher peak of curve "1" of Figure 4 is a result both of the higher initial pressure used in that test and the higher volume percentage of propane in air. (As shown in Reference 5, the maximum overpressure occurs at 5 percent by volume for propane in air.)

In order to fit the data shown in Figure 4 the following procedure was used.

1. A value of the exponent, m_e, of Equation (13) was chosen between 1.5 and 2.
2. The time of the occurrence of the peak, t_p, is obtained from the data (e.g., $t_p = 0.44$ for curve 2 of Figure 4).
3. The ratio of the peak pressure to the initial pressure (P/P_o) in an adiabatic constant volume burning is equal to the ratio of the adiabatic flame temperature to the initial temperature (T_f/T_w).
4. Using Equation (20) with procedures (2) and (3) above solves for the initial value of the flame speed:

$$V_{fo} = \frac{L}{t_p}\left[\frac{\left(\frac{T_f}{T_w}\right)^{\frac{(1 - m_e)(\gamma - 1)}{\gamma}} - 1}{\frac{(1 - m_e)(\gamma - 1)}{\gamma}\left(\frac{T_f}{T_w} - 1\right)}\right] \tag{24}$$

Using the above procedure the data of Table 1 were calculated. The data shown in Table 1 were calculated at 0.01 s time intervals from 0 s to 0.44 s. The last column of Table 1

TABLE 1

TIME HISTORIES OF VARIOUS PROPERTIES CALCULATED FROM THE ANALYTICAL SOLUTION WITHOUT HEAT LOSSES

EXPONENT m= 1.5 Vfo= 4.341 ft/s Tf=4050.0 deg-R Tw= 500.0 deg-R
Po= 17.14 psia L= 7.5 ft t-peak=0.44 s

t	dP	P	Tr	Tp	Rho/Rho0	Lp
0.00	0.00	17.14	500.00	500.00	1.000	0.00
0.01	0.72	17.86	505.92	3056.52	1.030	0.26
0.02	1.48	18.62	511.95	3077.44	1.061	0.52
0.03	2.27	19.41	518.09	3098.45	1.093	0.77
0.04	3.10	20.24	524.34	3119.57	1.126	1.01
0.05	3.97	21.11	530.70	3140.79	1.161	1.25
0.06	4.89	22.03	537.18	3162.10	1.196	1.48
0.07	5.85	22.99	543.78	3183.52	1.233	1.71
0.08	6.86	24.00	550.50	3205.04	1.272	1.94
0.09	7.92	25.06	557.34	3226.65	1.312	2.16
0.10	9.04	26.18	564.32	3248.36	1.353	2.37
0.11	10.21	27.35	571.42	3270.18	1.396	2.58
0.12	11.44	28.58	578.66	3292.09	1.441	2.78
0.13	12.74	29.88	586.04	3314.10	1.487	2.99
0.14	14.10	31.24	593.56	3336.20	1.535	3.18
0.15	15.54	32.68	601.23	3358.41	1.586	3.37
0.16	17.05	34.19	609.05	3380.71	1.638	3.56
0.17	18.64	35.78	617.02	3403.11	1.692	3.75
0.18	20.32	37.46	625.14	3425.61	1.748	3.93
0.19	22.09	39.23	633.43	3448.20	1.806	4.10
0.20	23.95	41.09	641.89	3470.90	1.867	4.27
0.21	25.91	43.05	650.51	3493.69	1.931	4.44
0.22	27.99	45.13	659.32	3516.59	1.997	4.61
0.23	30.18	47.32	668.30	3539.59	2.065	4.77
0.24	32.49	49.63	677.46	3562.69	2.137	4.93
0.25	34.93	52.07	686.82	3585.90	2.211	5.08
0.26	37.50	54.64	696.37	3609.21	2.289	5.23
0.27	40.23	57.37	706.12	3632.62	2.370	5.38
0.28	43.11	60.25	716.07	3656.15	2.455	5.53
0.29	46.16	63.30	726.24	3679.79	2.543	5.67
0.30	49.39	66.53	736.63	3703.54	2.635	5.81
0.31	52.80	69.94	747.24	3727.41	2.730	5.94
0.32	56.42	73.56	758.09	3751.39	2.831	6.08
0.33	60.25	77.39	769.17	3775.50	2.935	6.21
0.34	64.31	81.45	780.49	3799.74	3.044	6.34
0.35	68.62	85.76	792.07	3824.10	3.159	6.46
0.36	73.19	90.33	803.90	3848.60	3.278	6.59
0.37	78.04	95.18	816.01	3873.23	3.403	6.71
0.38	83.19	100.33	828.39	3898.01	3.533	6.83
0.39	88.66	105.80	841.05	3922.94	3.670	6.95
0.40	94.48	111.62	854.01	3948.02	3.813	7.06
0.41	100.66	117.80	867.26	3973.26	3.962	7.17
0.42	107.24	124.38	880.83	3998.66	4.119	7.28
0.43	114.24	131.38	894.72	4024.24	4.283	7.39
0.44	121.69	138.83	908.94	4050.00	4.456	7.50

gives the position, L_p, of the flame at the value of time shown in the first column. The position is calculated from the equation

$$\frac{L_p}{L} = 1 - \quad 1 - \frac{m_p}{m} \frac{v_u}{v_o} \tag{25}$$

It is of interest to plot the overpressure given in column 2 versus the relative flame position L_p/L as shown in Figure 5. We have referred to the relative flame position as the void fraction since in the flame suppression tests the flame tube is packed with foam from some position in the flame tube to the end of the tube. The volume in front of the foam over the total volume of the tube is referred to as the void fraction. If a flame traveled up to the position of the foam and was extinguished at that point, the value of the overpressure achieved would be given by the curve shown in Figure 5. This concept will be compared to experimental results in a later section.

The overpressure shown in Table 1 is plotted versus time in Figure 6 where it is compared to the data shown in Figure 4. The comparison is reasonably good for both curves. The peak value is higher than the experimental value by about 11 percent which is probably due to neglecting the heat transfer. The effects of heat transfer will be discussed in a later section. However, in the next section we will first develop a theory for the flame arrestor tests and compare the results to experiments.

FLAME ARRESTOR TESTS

Figure 7 shows the configuration of the flame tube for flame arrestor testing. The front of the foam is located 15 inches from the front of the flame tube which gives a combustion void of 16.7 percent. The region behind the foam is the relief volume. The thickness of the foam used in the test varies from 5 inches down to 0.5 inch or the smallest thickness of foam that

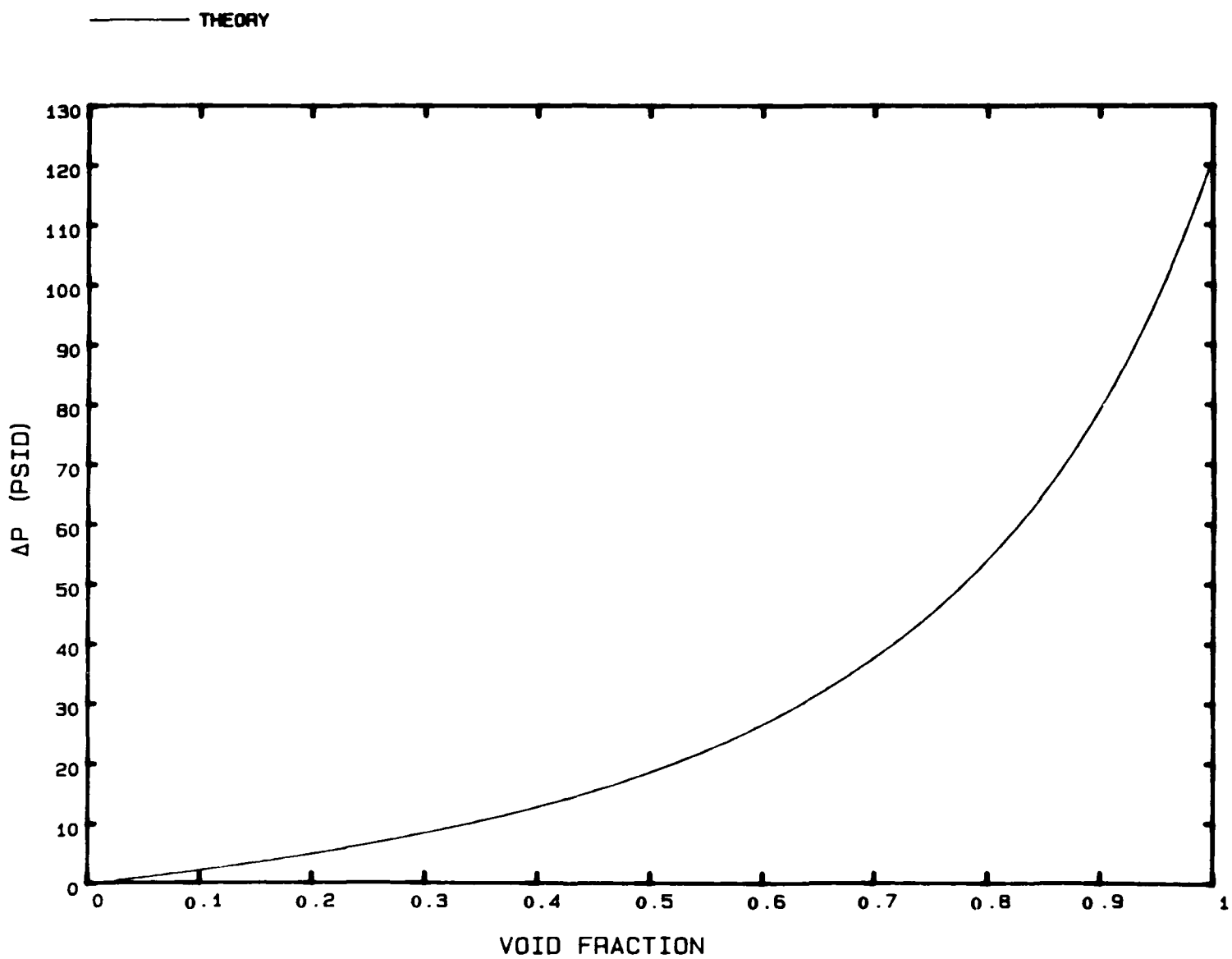

Figure 5. Overpressure versus void fraction (LP/L = void fraction).

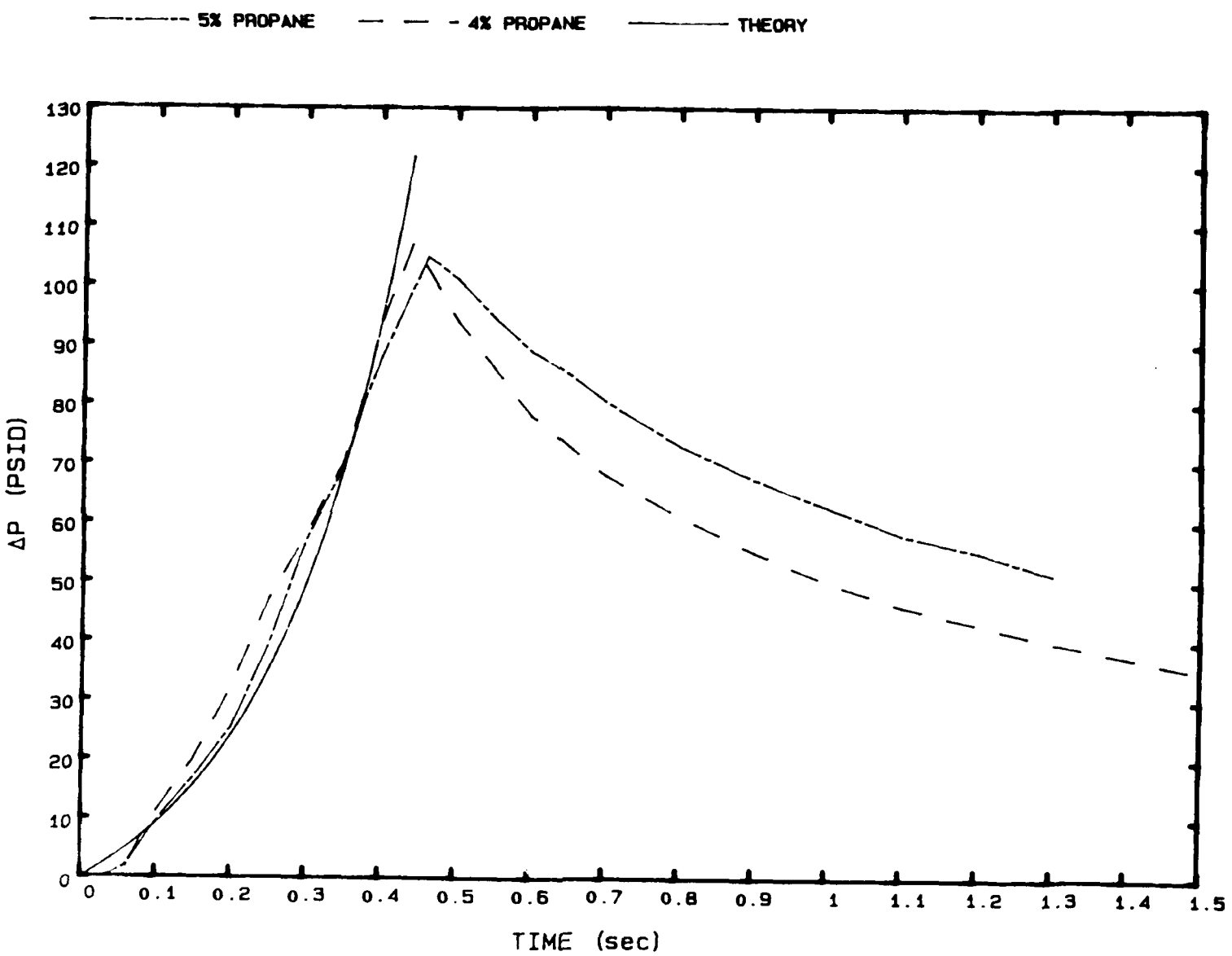

Figure 6. Theoretical overpressure compared to experimental data.

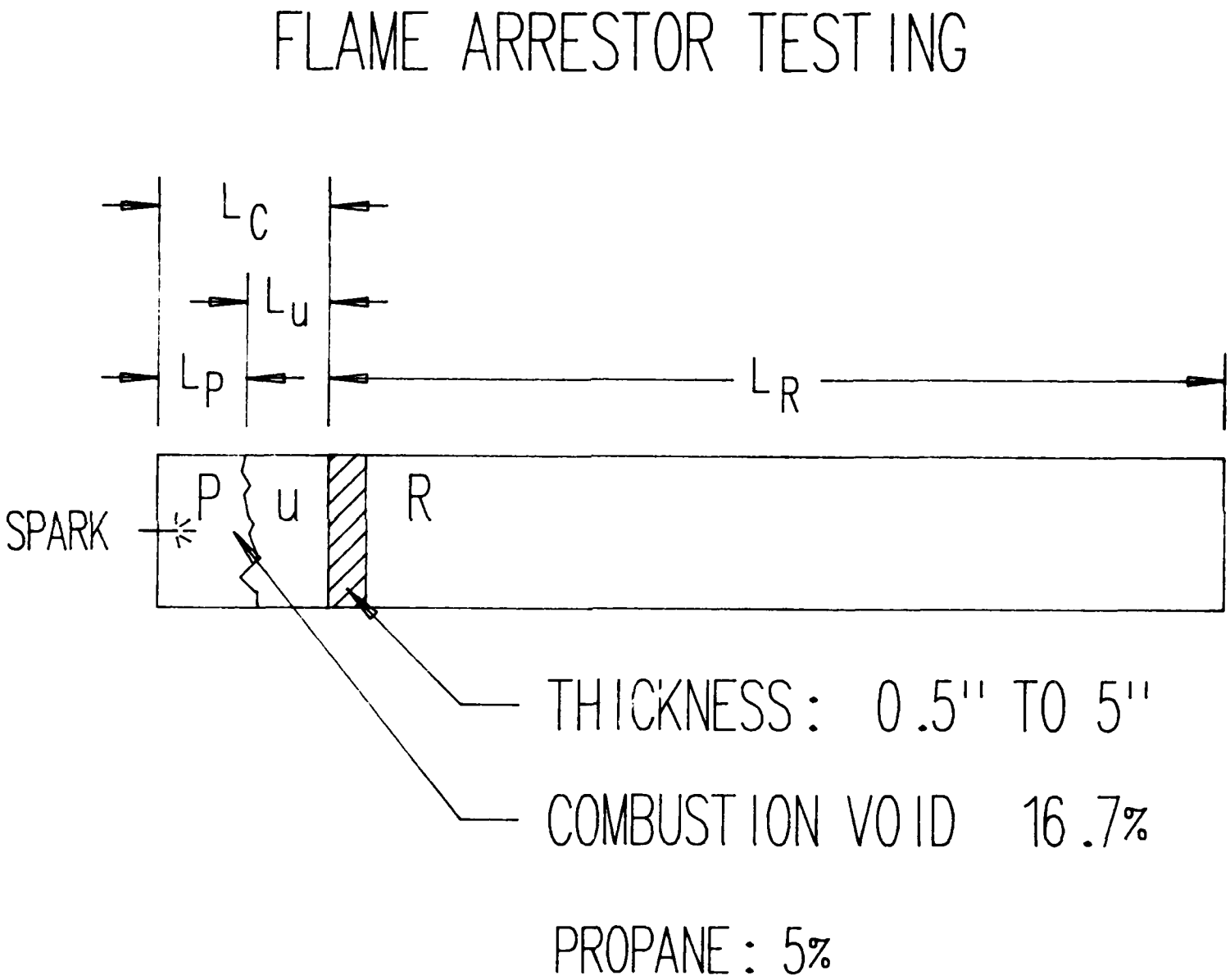

Figure 7. Configuration of flame tube for flame arrestor testing.

does not blow through. During the burning the flame front drives the combustion void into two regions: one contains the products of combustion and the other contains the unburnt mixture.

Two extreme effects of the foam can be considered. The first extreme case is represented by a foam that does not prevent the transmission of the pressure waves through the foam but extinguishes the flame when it reaches the foam. In this case the overpressure would be about 4 psid which can be obtained from Figure 5 at a void fraction of 16.7 percent.

In the other extreme case all of the pressure waves would be reflected by the foam (it would act like a solid wall) and the pressure would reach the peak value consistent with adiabatic constant volume burning.

It was believed that the foam acted somewhere between these two extremes and would show a resistance that would increase the overpressure in front of the foam above the value shown at 16.7 percent void fraction in Figure 5. A theory was developed for this case, which is similar to one developed in Reference 6, as follows. However the experimental results, as discussed later, show that foam does not substantially attenuate pressure waves and therefore, the first extreme case is essentially what occurs.

The conservation of mass for a control volume in front of the foam leads to an equation similar to Equation (5):

$$\frac{m_P}{m} \frac{T_P}{T_u} - 1 = \frac{v_o}{v_u} - 1 + \int_o^t \frac{\dot{m}_f dt}{m_{uo}} \tag{26}$$

where $\dot{m}_f$ is the mass flow rate through the foam and the integral gives the total mass flow out of the region in front of the foam during the time t.

When the energy equation for the control volume is combined with Equation (26), the resulting expression for the pressure is

$$\frac{d\left(\frac{P}{P_o}\right)}{dt} = \left(\frac{T_f - T_w}{T_w}\right)\frac{d\left(\frac{m_P}{m_{uo}}\right)}{dt} - \gamma\,\frac{T_u}{T_w}\,\frac{\dot{m}_f}{m_{uo}} + \frac{\dot{Q}_T}{m_{uo}C_vT_w} \tag{27}$$

It can be shown that the flow from a reservoir through a pipe with and without foam in the pipe leads to tne equation

$$\dot{m}_f = \dot{m}_{fi}/\sqrt{1 + f_{TOT}} \tag{28}$$

where $\dot{m}_{fi}$ is the mass flow rate for an inviscid case (i.e., no foam) and f_{TOT} is the total friction factor of the foam. The mass flow rate at any location in the flame tube without foam can be related to the time rate of change of the pressure as follows.

$$\frac{\dot{m}_{fi}}{m_{uo}} = \frac{1}{\gamma}\,\frac{L_R}{L_c}\,\frac{T_w}{T_u}\,\frac{d\left(\frac{P}{P_o}\right)}{dt} \tag{29}$$

Combining Equations (27), (28), and (29) leads to

$$\frac{d\left(\frac{P}{P_o}\right)}{dt} = \frac{\left(\frac{T_f - T_w}{T_w}\right)\frac{d\left(\frac{m_P}{m_{uo}}\right)}{dt} + \frac{\dot{Q}_T}{m_{uo}C_vT_w}}{\left(1 + \frac{L_R}{L_c\sqrt{1 + f_{TOT}}}\right)} \tag{30}$$

Equation (30) reduces to Equation (19) if both L_R and $\dot{Q}_T$ are zero.

The pressure behind the foam is related to the mass flow into the region R by Equation (29) if P is replaced by P_R and $\dot{m}_{fi}$ is replaced by $\dot{m}_f$. It follows that

$$\frac{d\left(\frac{P_R}{P_o}\right)}{dt} = \frac{1}{\sqrt{1 + f_{TOT}}} \frac{d\left(\frac{P}{P_o}\right)}{dt} \tag{31}$$

Since Equation (18) is still valid, Equations (30) and (31) can be solved for zero heat transfer. Results from the solution are shown in Figure 8. The theoretical pressure rise in front of the foam would depend on the thickness of the foam since f_{TOT} in the equations above is directly proportional to the foam thickness. As seen from Figure 8, the pressure in front of the foam is predicted to be substantially higher than the pressure behind the foam when we use values of f found with the pressure drop rig.

We first compared the theory to data obtained from Reference 2. The data points plotted between 0.5 and 2 inches in Figure 8 are from Reference 2 for Crest type III red foam. Although two pressure transducers were used in the tests, they were located behind the foam and therefore, the results were not contradictory to the theory.

In order to conduct definitive tests we ran tests with 3 and 5 inch thick pieces of foam. The pressure transducers were relocated so that one was in front of the foam and the other was behind the foam. The results of these tests are also plotted in Figure 8.

These tests demonstrated convincingly that the foam does not hinder the passage of pressure waves through it since both transducers had essentially the same time histories. Therefore the peak pressure, provided the flame is extinguished by the foam, can be predicted reasonably well from the location of the foam using Figure 5.

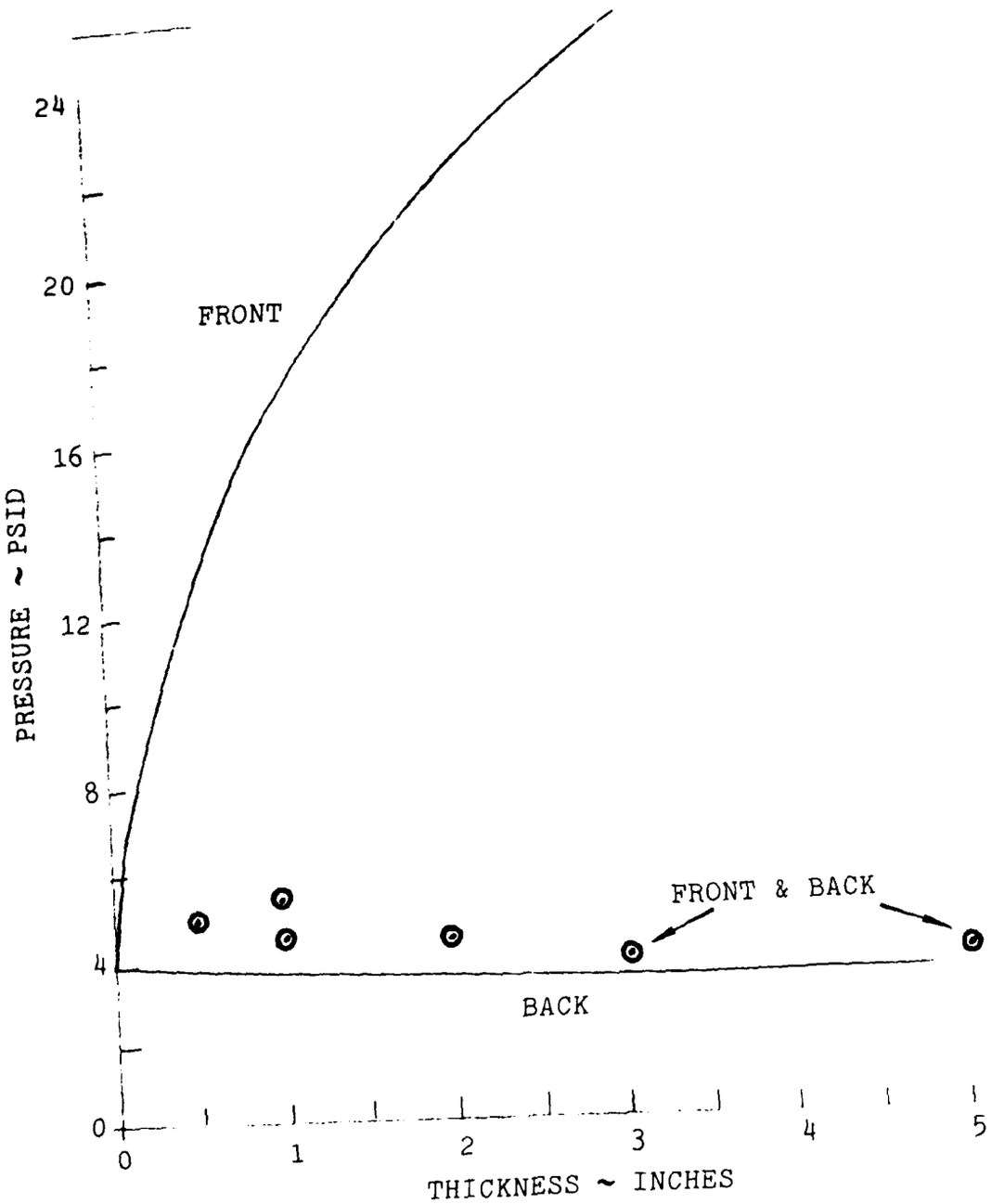

Figure 8. Predicted pressures in front of the foam and behind the foam for the flame arrestor tests.

It should be pointed out that the minimum foam thickness that will extinguish the flame is fairly thin. Therefore, the method used to support the foam in these tests has a significant effect on the results. Tests reported in Reference 2 showed erratic results until it was determined that one of two racks being used gave inadequate support of the foam. After this rack was discarded, the results were consistent and foam extinguished the flame even when tested down to a one-half inch thickness.

In the next section results of the explosion suppressant testing will be compared to the theory.

EXPLOSION SUPPRESSANT TESTS

Figure 9 shows a schematic of the flame tube configuration used for explosion suppressant tests. In these tests various combustion voids are tested by packing various amounts of foam into the flame tube.

Results from a number of tests described in Reference 2 are shown plotted in Figure 10 where the peak overpressure is plotted versus void fraction. The data are compared to the theoretical curve shown in Figure 5.

In Figure 10 two test series of Crest type II red foam are shown. In the first series tests were run with racks present in the void space in front of the foam. As seen in Figure 10, the results were very erratic with some very high overpressures. The data for the other two types of foam were also obtained with the racks present but each of these foams was qualified under Military Specification MIL-B-83054B (USAF). Therefore these two types were not rerun without racks.

After the initial tests for the type III foam were run with the racks, it was determined that earlier qualification tests were run on other foams without the racks present. Apparently the racks moved during the test and compressed the foam which enlarged the combustion void and consequently increased the

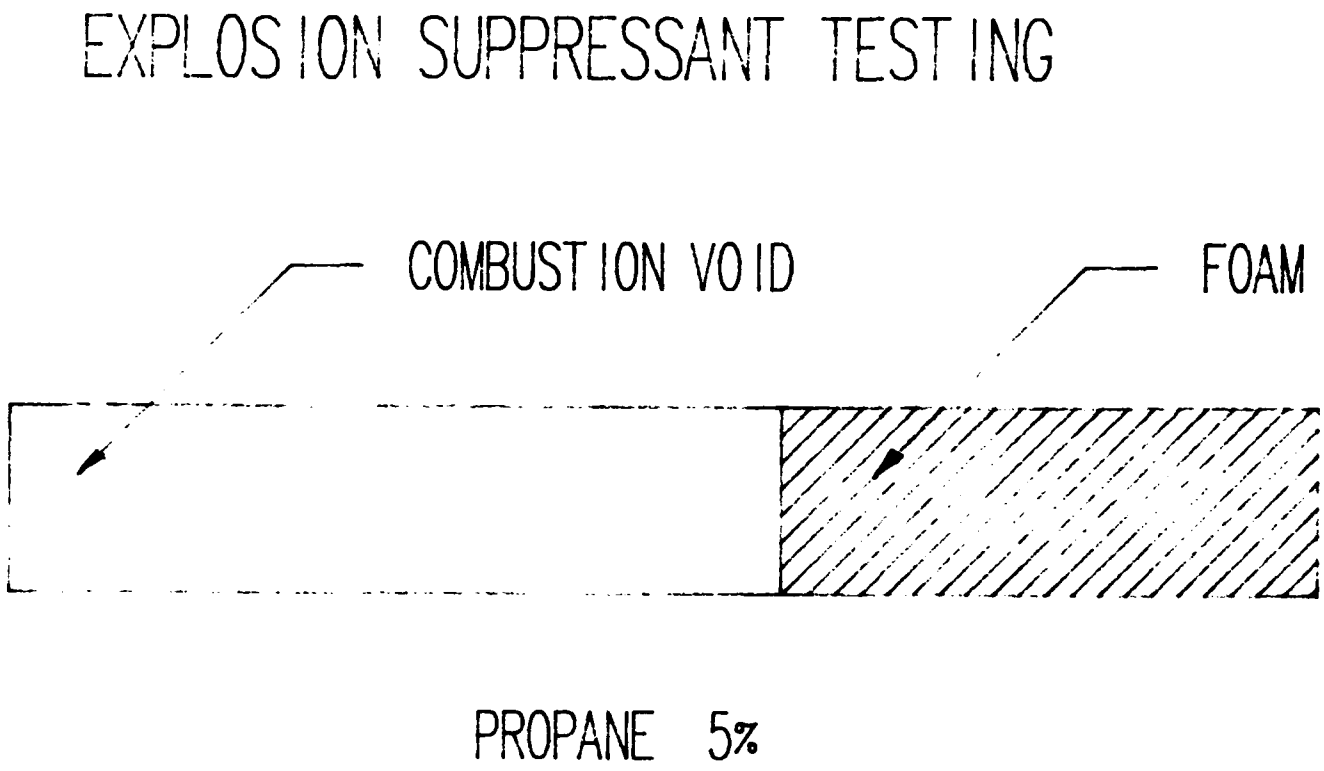

Figure 9. Configuration of flame tube for explosion suppressant testing.

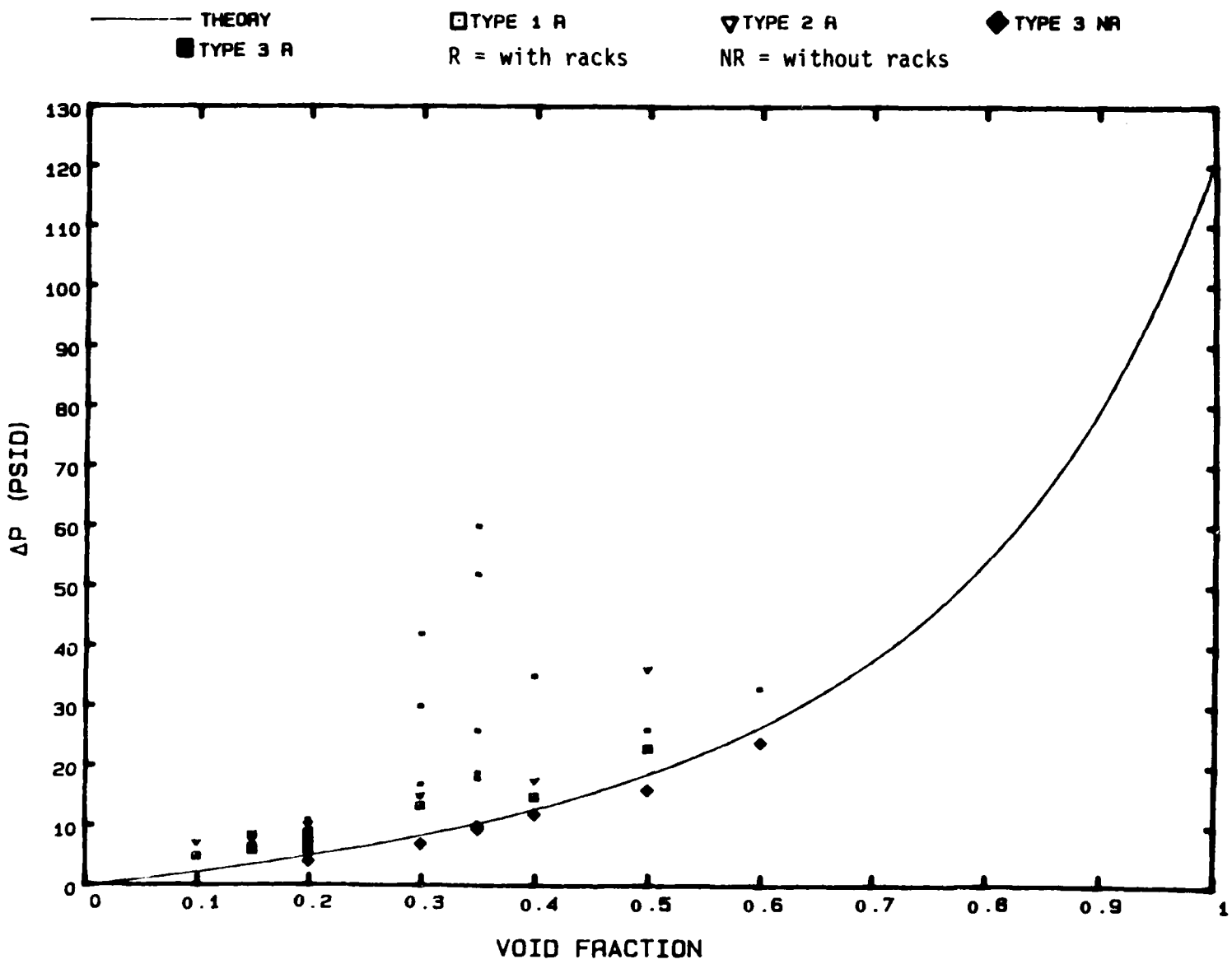

Figure 10. Overpressure data compared to theory for three types of foam.

overpressure. Subsequently the qualification tests for the type III foam were rerun without the racks in the combustion void.

As can be seen in Figure 10, the results were no longer erratic and they agreed very well with the theory developed earlier. Because of these results it was decided to rerun one of the other foams without racks to see if the results would more nearly agree with the theory. The type I orange foam was chosen for testing without racks and the results are shown in Figure 11 where both the type III and type I results without racks are shown.

At combustion voids of 50 percent or less the results are in excellent agreement with the theory. Above 50 percent the one point for the type III red foam still agrees quite well with the theoretical curve while the two points shown for the type I foam show a higher peak pressure than the theory would predict. This may be because the foam did not extinguish the flame and burning continued into the foam. This phenomena is not uncommon in the explosion suppressant testing and was observed on a number of occasions during testing.

The type I orange foam is the most open foam with a nominal 10 pores per inch and was chosen for retesting because of this. The type III red foam has a nominal 25 pores per inch and therefore, has a smaller pore size than the type I orange foam. The type I orange foam would allow the flame to penetrate the foam more readily than the type III red foam.

The larger combustion voids bring the mixture within the foam to a higher pressure and temperature before the flame reaches the foam. This preheating may permit the flame to penetrate into the foam and increase the peak pressures in the tests at the higher values of combustion void. The data for the type I orange foam are commensurate with this concept. The type III red foam, because of its smaller pores, would require more preheating than the type I orange foam. This may explain why the type III red foam still agrees with the theory at a combustion

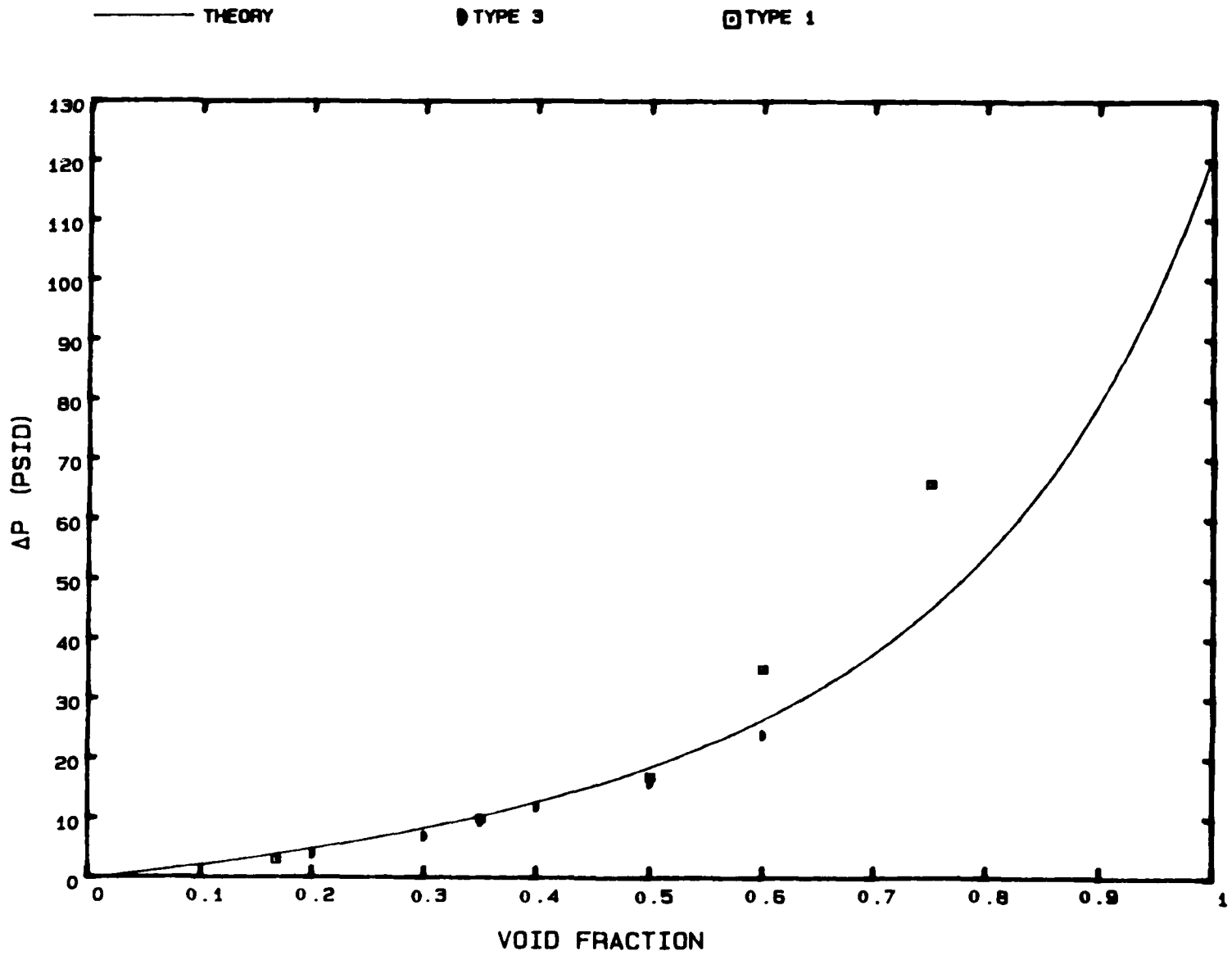

Figure 11. Comparison of experimental data to theory for two types of foam. Test data taken without racks present in the void space.

void of 60 percent while the type I orange foam exhibits an increase in overpressure over the theory at a combustion void of 60 percent as shown in Figure 11.

In order to extend the theory to investigate the propagation of the flame into the foam it is necessary to consider the effects of heat transfer.

HEAT LOSS STUDY

When the effects of heat transfer are considered, the heat loss terms in Equations (11) and (16) must be retained. A closed form solution was not found for this case, but a fourth-order Runge-Kutta numerical procedure was used to solve Equations (14), (16), and (19) (a heat transfer term was added to Equation (19)). The method was checked with the exact solution by setting the heat transfer to zero. The heat transfer term, required in Equation (19), is obtained from Equation (11) by differentiating with respect to time. The result is

$$\frac{d\left(\frac{P}{P_o}\right)}{dt} = \frac{T_f - T_w}{T_w} \frac{d\left(\frac{m_P}{m}\right)}{dt} + \frac{\dot{Q}}{C_u m T_w} \tag{32}$$

The heat transfer term in Equation (32) is the total value and includes the heat loss from the products and from the unburnt reactants ($\dot{Q}_u$ of Equation (16)). The standard thermodynamics convention was used for the heat transfer terms: heat into the control volume is positive. The heat transfer from the unburnt reactants is

$$\dot{Q}_u = h_u^*(C_{iR}\ L_u)(T_w - T_u) \tag{33}$$

Hence, the term needed for Equation (16) is

$$\frac{\dot{Q}_u}{C_P T_w m_u} = \frac{h_u^*\ C_{iR}}{\gamma C_v \rho_{uo} A_t} \frac{\rho_o}{\rho_u}\left(1 - \frac{T_u}{T_w}\right) \tag{34}$$

The density ratio can be eliminated in favor of the temperature and pressure ratios resulting in

$$\frac{\dot{Q}_u}{C_p T_w m_u} = \frac{1}{\gamma}\left[\frac{h_u^* C_{iR}}{C_v \rho_{uo} A_t}\right]\frac{T_u}{T_w}\frac{P_o}{P}\left(1 - \frac{T_u}{T_w}\right) \tag{35}$$

In a similar way the heat transfer term needed for Equation (32) can be obtained

$$\frac{\dot{Q}}{C_v m T_w} = \left[\frac{h_P^* C_{iR}}{C_v \rho_{uo} A_t}\right]\frac{L_P}{L}\left(1 - \frac{T_P}{T_w}\right) + \left[\frac{h_u^* C_{iR}}{C_v \rho_{uo} A_t}\right]\frac{L_u}{L}\left(1 - \frac{T_u}{T_w}\right) \tag{36}$$

The terms in square brackets contain the heat transfer coefficients for each region and a geometric parameter (C_{iR}/A_t) which is related to the hydraulic diameter ($D_h = 4A_t/C_{iR}$). Thus, for example

$$\frac{h_P^* C_{iR}}{C_v \rho_{uo} A_t} = \frac{4h_P^*}{C_v \rho_{uo} D_h} \tag{37}$$

which shows the significance of the hydraulic diameter and consequently the small pore sizes in increasing the heat transfer. For small enough values of D_h the effect of the cooling is so large that the flame is quenched. If the flame is not quenched, the effect of the cooling for small D_h is to reduce the overpressure substantially as occurs in the explosion suppression foams when flame propagates through the foam.

In the above equations the heat transfer coefficient, h^*, is a function of temperature and can be a result of both free convection and radiation. For gray body radiation the value of h^* in BTU/hr/ft^2/°R is

$$h^* = 0.172 \times 10^{-8} \varepsilon T_w^3 \left(1 + \frac{T}{T_w}\right)\left(1 + \left(\frac{T}{T_w}\right)^2\right) \tag{38}$$

The results of using Equation (38) with various values of the emissivity, ε, are shown in Figures 12 through 16 where the theory is compared to the experimental data. The page parameter is the initial flame speed which varies from 4 ft/s for Figure 12 to 6 ft/s for Figure 16 in steps of 0.5 ft/s. The best fits are obtained with a flame speed of about 5 ft/s and ε of about 0.3. However, when compared to the data, the rate of cooling appears to be too high during the pressure rise phase and not high enough during the cooling phase.

In an attempt to obtain a better fit to the data the gas radiation theory developed by Hottel and Egbert (References 7, 8, and 9) was used. They present a series of charts to account for the radiation due to water vapor and carbon dioxide. These charts are widely used to determine the emissivity of gases.

The following equations, which approximate the charts, were given by Ganapathy in Reference 10 to approximate ε.

$$\varepsilon = 0.9(1 - e^{-KL_b}) \tag{39}$$

where

$$K = (0.8 + 1.6\ P_w)(1 - 0.38T/1000)\sqrt{(P_c + P_w)L_b} \tag{40}$$

and

$$L_b = 3.4\ A_t L/L \cdot C_{iR} = 3.4\ D_h/4 \tag{41}$$

In Equations (39) through (41) T is the temperature in Kelvin, P_c and P_w are the partial pressures of carbon dioxide and water vapor in atmospheres, and L_b is the beam length in meters.

A term was also added to account for free convection.

$$h^*_{fC} = C\ \frac{k}{L}\left(\frac{g\beta(T - T_w)L^3\rho^2 C_v}{\mu k}\right)^{1/4} \tag{42}$$

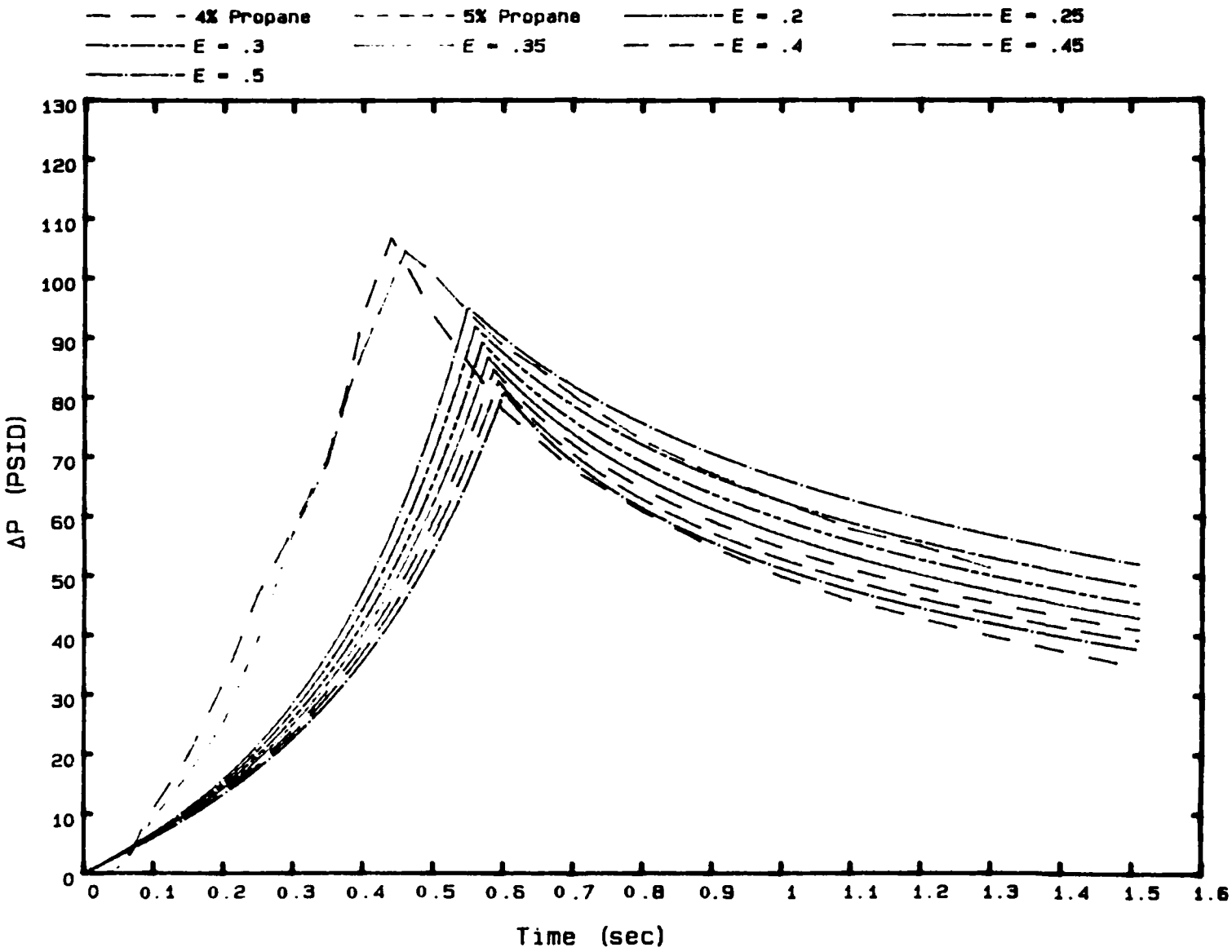

Figure 12. Pressure versus time with gray body radiation curves for various values of ϵ. The initial flame speed is 4 ft/s.

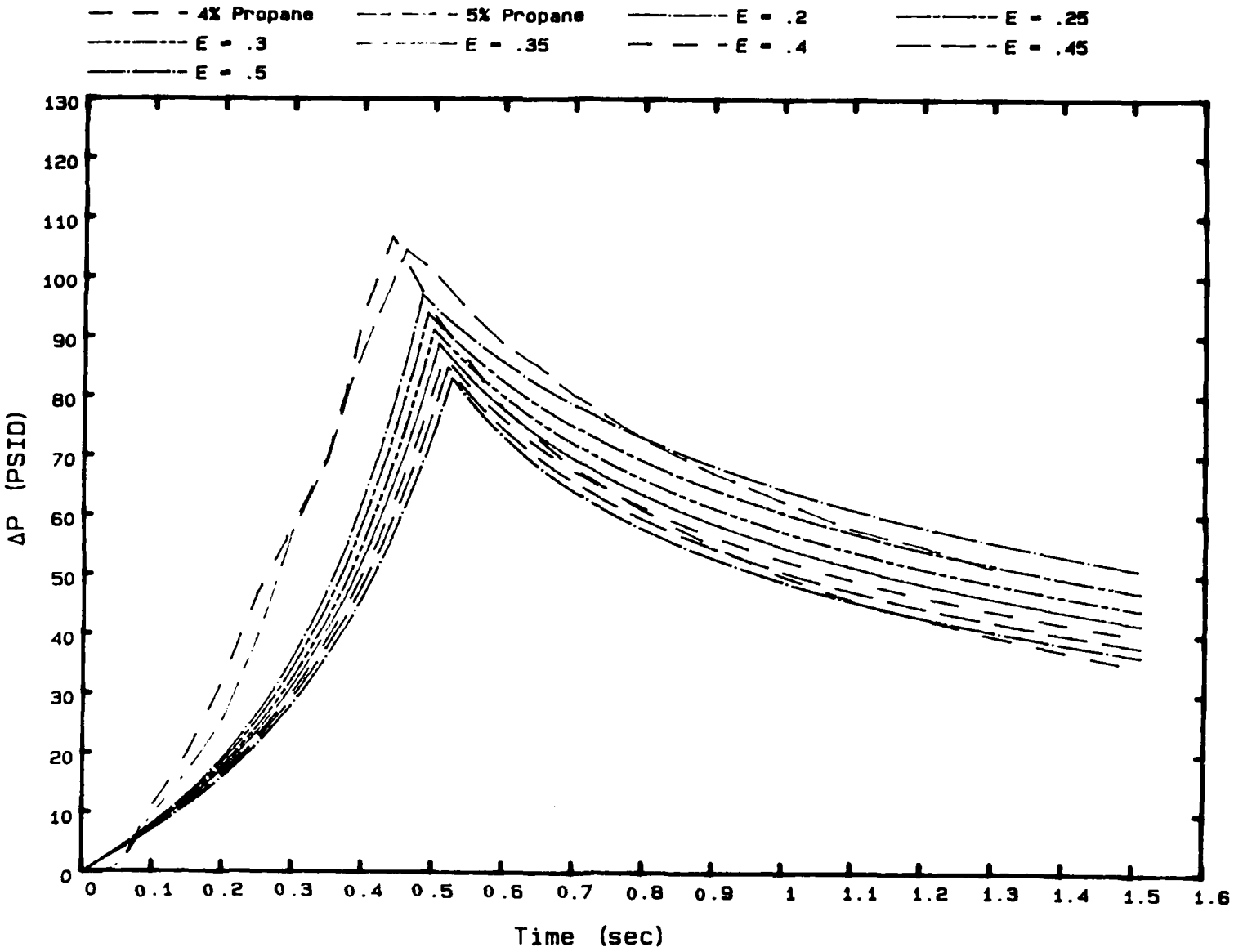

Figure 13. Pressure versus time with gray body radiation curves for various values of ϵ. The initial flame speed is 4.5 ft/s.

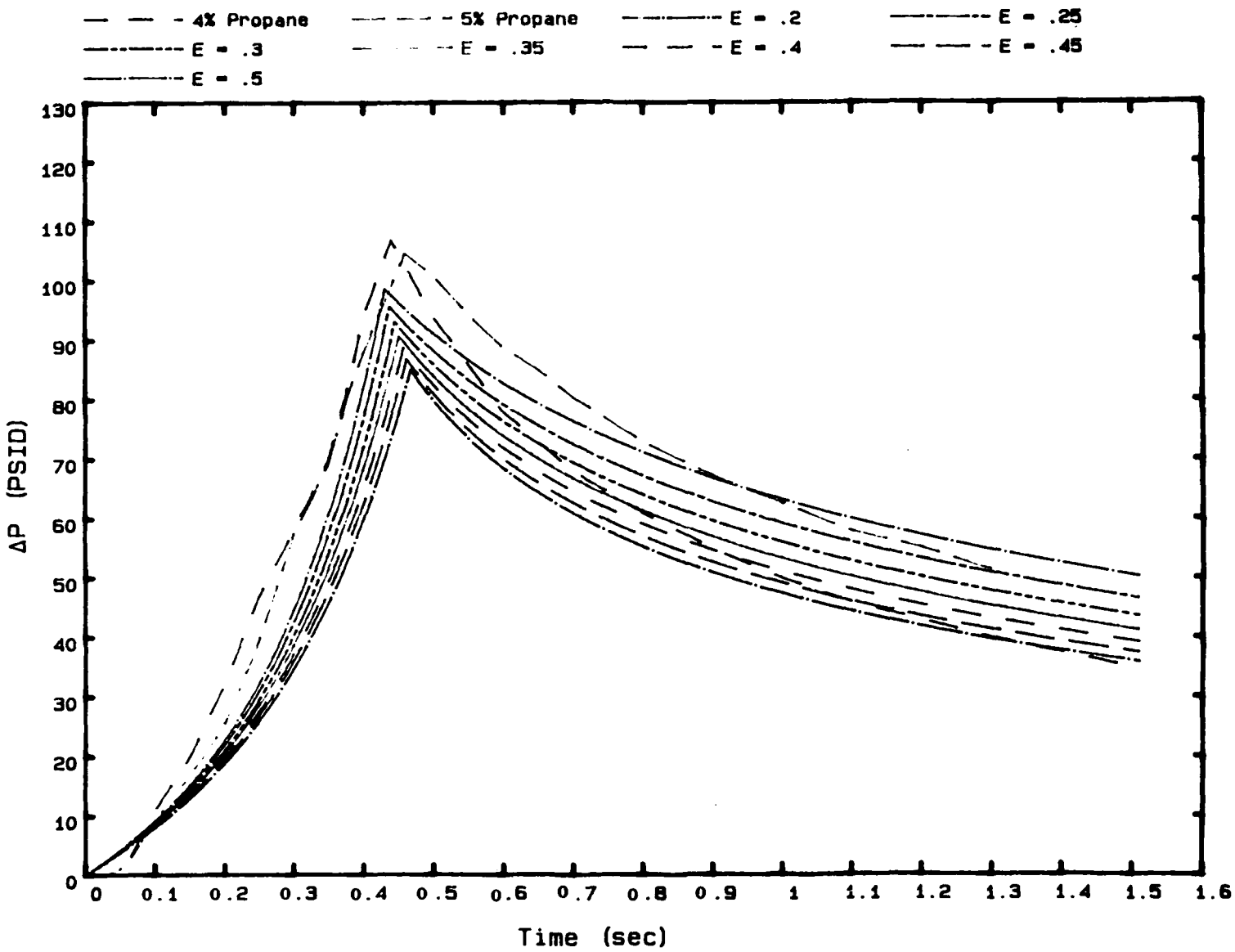

Figure 14. Pressure versus time with gray body radiation curves for various values of ϵ. The initial flame speed is 5 ft/s.

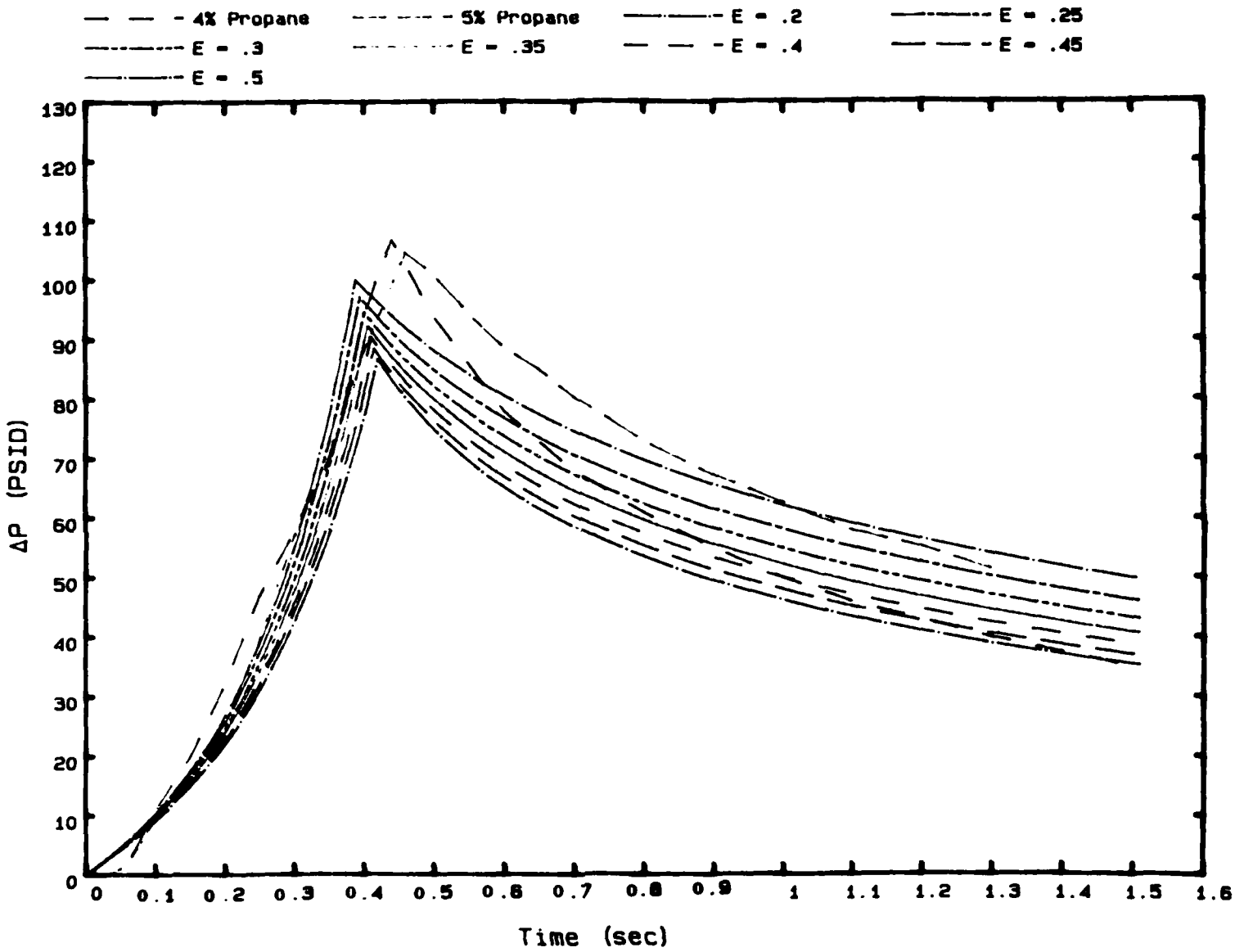

Figure 15. Pressure versus time with gray body radiation curves for various values of ϵ. The initial flame speed is 5.5 ft/s.

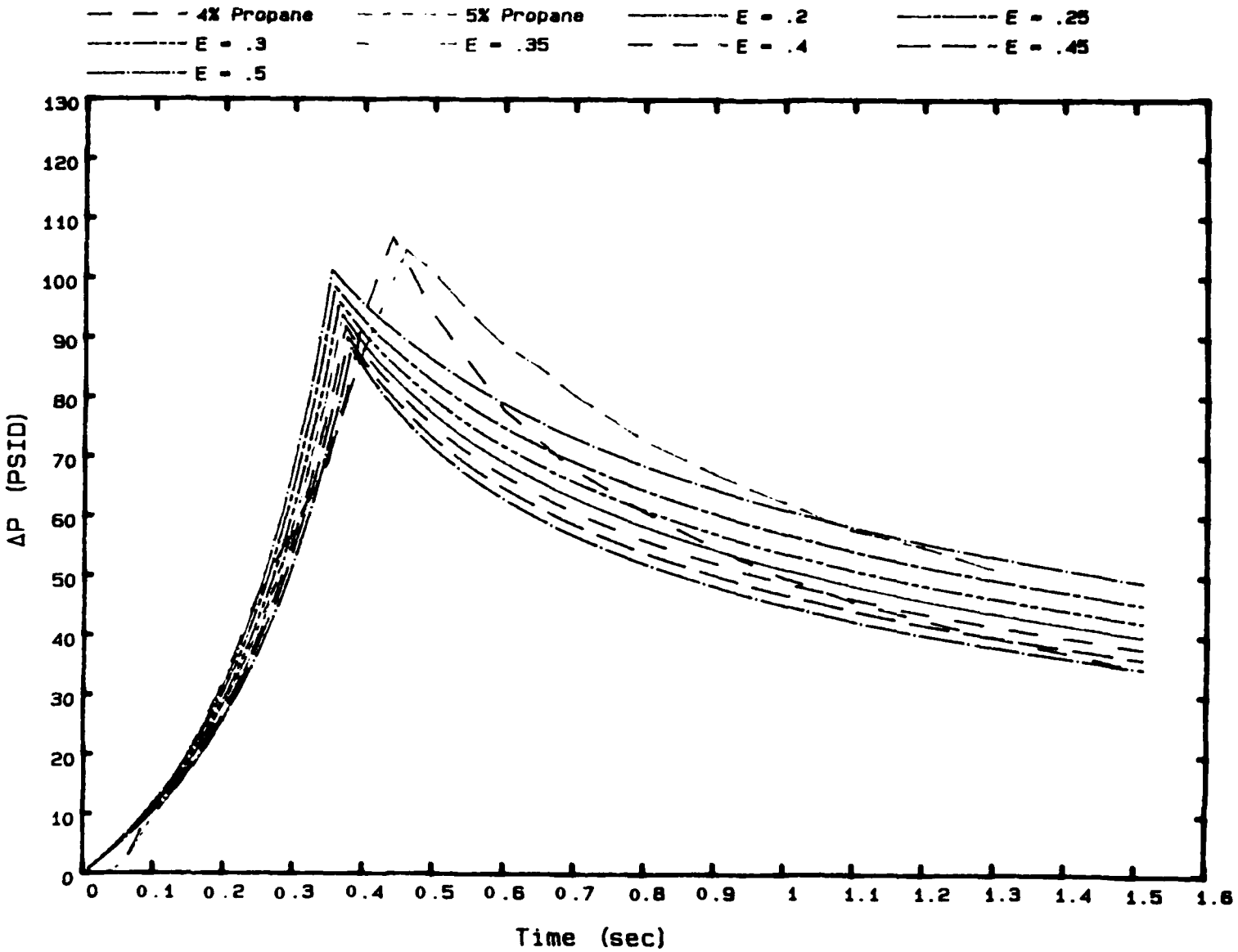

Figure 16. Pressure versus time with gray body radiation curves for various values of ϵ. The initial flame speed is 6 ft/s.

Using the well known Sutherland formula for μ and k and recalling that β is 1/T for an ideal gas yields

$$h^*_{fC} = \left[C\frac{k_o}{L}\left(\frac{gL^3\rho_o{}^2C_v}{\mu_o k_o}\right)^{1/4}\right]\left(\frac{T}{T_w} - 1\right)^{1/4}\sqrt{\frac{1.45\ \frac{T}{T_w}}{\left(\frac{T}{T_w} + .45\right)}} \tag{43}$$

Using a value of C = 0.55 and substituting for the various values yields a value of 1.3 for the term in square brackets if h^*_{fC} is in BTU/hr/ft^2/°R.

The results of the above approach are seen in Figure 17 where the theory is compared to experiment. The fit shown was for a flame speed of 4.34 ft/s. The cooling does not follow the data very well and apparently the value of h^* is too small.

The gas radiation theory used was originally substantiated by experiments at high gas temperatures. Therefore, it is believed that the heat transfer from convection must be substantially higher than that predicted from Equation (43). Since a purely theoretical approach did not yield satisfactory results, an emperical fit was obtained using the equation

$$h^* = C(T - T_w)^m \tag{44}$$

During the cool down phase the temperature of the products can be determined from the following equation.

$$\frac{dT}{dt} = -\left[\frac{4h^*}{C_v\rho_o D_h}\right](T - T_w) \tag{45}$$

Substitution of Equation (44) in Equation (45) yields

$$\frac{dT}{dt} = -\left[\frac{4C}{C_v\rho_o D_h}\right](T - T_w)^{1 + m} \tag{46}$$

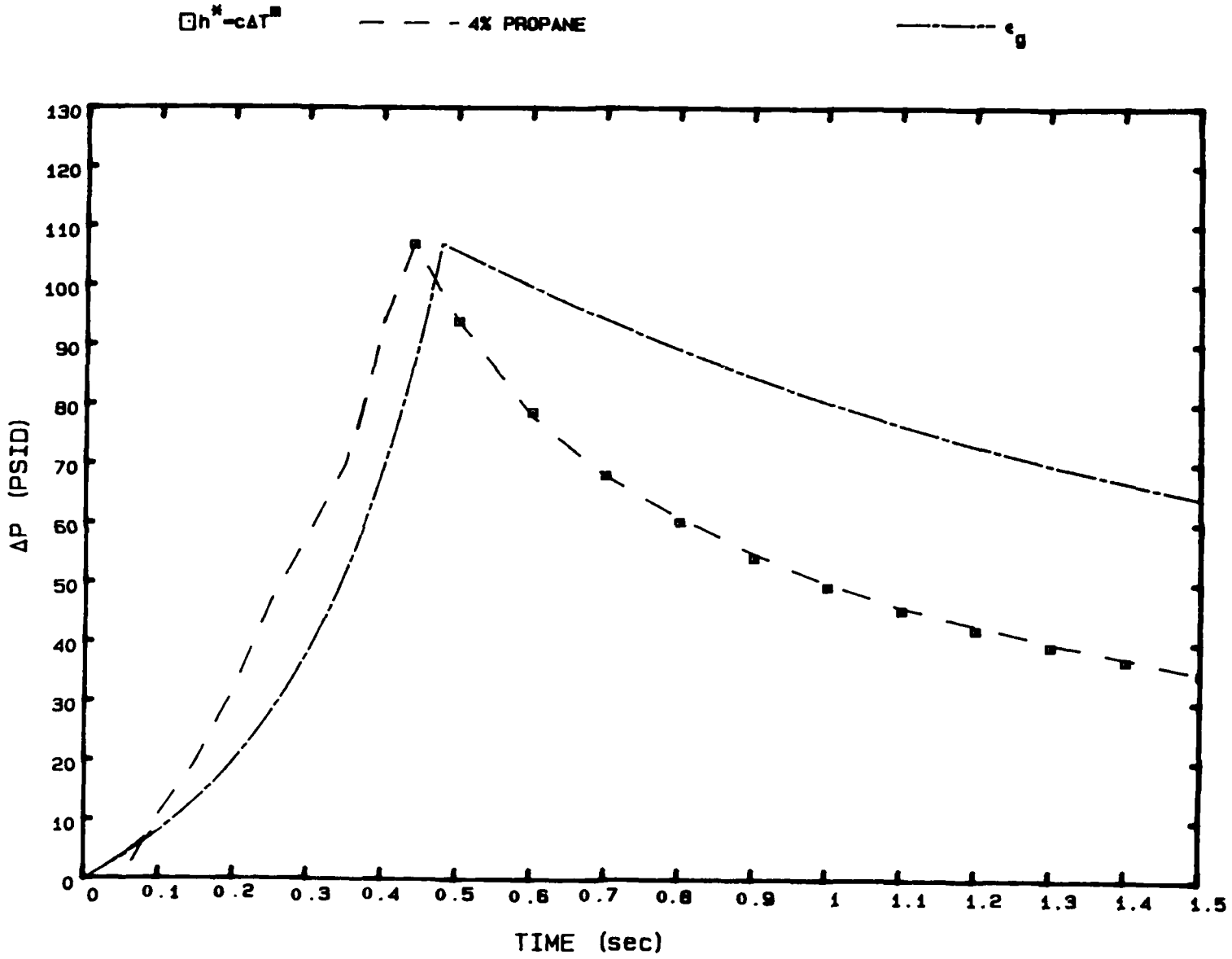

Figure 17. Comparison of the theory with heat loss to experiment. Also shown are data points for the empirical fit to the cool down phase.

In view of Equation (44) we can eliminate C in favor of the initial value of heat transfer coefficient h_i^*.

$$\frac{dT}{dt} = -\left[\frac{4h_i^*}{C_v \rho_o D_h}\right] \frac{(T - T_w)^{1 + m}}{(T_i - T_w)^m} \tag{47}$$

The solution to Equation (47) is

$$\frac{T}{T_w} = \frac{P}{P_o} = 1 + \frac{\frac{P_i}{P_o} - 1}{\left(1 + m \frac{4h_i^*}{C_v \rho_o D_h} \Delta t\right)^{1/m}} \tag{48}$$

By trial and error a fit of Equation (48) was made to the cool down data and is also shown in Figure 17. The fit to the data was excellent for a value of m = 1.2795 and h_i^* = 33.39 BTU/hr/ft^2/°R (or C = 0.001129). The value of P_i/P_o as read from the data was 7.24.

Although time was not available under the current contract, Equation (44) should be used along with the hydraulic diameter of the various foams to study the effects of burning within the foam and for determining when the flame will be extinguished by the foam. The relationship for determining the pore size required for extinguishing the flame will be discussed in the next section.

PORE SIZE CORRELATION WITH PRESSURE DROP

In determining if a foam will extinguish a flame or if a flame will propagate into the foam it is necessary to determine the pore size of the foam.

A criteria for extinguishing a flame was presented by Wilson and Attalah in Reference 11. Flame quenching is related

to the hydraulic diameter as would be anticipated from the heat loss study presented above. This quenching only occurs if the hydraulic diameter is less than a critical value, D_h^*.

Wilson and Attalah relate D_h^* to the thermal diffusivity α, laminar flame speed V_ℓ, and the Peclet number, N_{Pe}:

$$D_h^* = N_{Pe} \frac{\alpha}{V_\ell} \tag{49}$$

According to Wilson and Attalah for hydrocarbon-air mixtures at standard conditions a typical value of Peclet number is 60. Therefore the critical hydraulic diameter for many fuels is

$$D_h^* = 60 \frac{\alpha}{V_\ell} \tag{50}$$

Reference 4 develops a similar expression for D_h^*. The idea of a minimum diameter below which a fuel-air mixture cannot support a flame is so widely accepted that the "quenching diameter" is often listed with the flame speed as a fundamental property of the fuel. Both Reference 11 and 4 give values of 0.25 cm (0.1 in) as typical values of hydrocarbon fuel. (Note that Reference 11 suggests that distances cited in the literature for parallel plates or slots be multiplied by 1.4 to obtain the hydraulic diameter.)

For propane Reference 11 gives a value of 0.24 cm for D_h^*. They also suggest for fuel-air mixtures having laminar flame speeds up to 100 cm/s (3.3 ft/s) that a conservative design criterion is

$$D_h^* \leq 0.075 \text{ cm } (0.03 \text{ in})$$

which has a safety factor of two or more, depending on the fuel (hydrogen and acetylene may require smaller values of D_h^*).

The value of D_h^* depends on the pressure and the temperature of the unburnt reactants. For hydrocarbon fuels burning in air the following adjustments to D_h^* should be made:

$$D_h^* = D_{h_o}^* \frac{P_o}{P} \sqrt{\frac{T_{uo}}{T_u}} \tag{51}$$

For propane the value of $D_{h_o}^*$ is 0.24 cm for P_o equal to 1 atmosphere and T_{uo} at a temperature of 80°F. Equation (51) can be used to adjust D_h^* to other conditions.

The hydraulic diameter of the foam can be estimated from the formula

$$D_h = \frac{4 \cdot \text{volume}}{\text{surface area}} = \frac{4\ \text{Vol}}{A_s} = \frac{4}{S} \tag{52}$$

The surface area to volume ratio, s, is the specific surface area of the foam. For foam with a density of 1.75 pounds per cubic foot Scott (form 3645-R-0375) shows the variation of the specific surface area as a function of the pores per inch. A satisfactory fit to their data is

$$S = 9.64\ P_{pi}^{1.169} \tag{53}$$

where S has units of ft^2/ft^3 and P is in pores per inch. Thus, in view of Equation (52) an estimate of the hydraulic diameter is

$$D_h = 0.4149\ P_{pi}^{-1.169} \tag{54}$$

where D_h is in feet. If the constant 0.4149 is replaced by 1.960, the result would be in centimeters. If Equation (54) is used to calculate the hydraulic diameter of the type I orange foam (10 pores per inch) and the type III red foam (25 pores per inch), the result is 0.133 cm and 0.0455 cm, respectively. Thus, both foams have hydraulic diameters less than the 0.24 cm value for D_h^* at 1 atmosphere and 80°F. However, if the value of D_h^* is

adjusted by Equation (51) using the data of Table 1, then the result can be plotted as shown in Figure 18. Figure 18 shows the variation in D_h^* in centimeters as the flame progresses down the flame tube. When the flame has traveled to 4.5 feet (60 percent of 7.5), the new value of D_h^* is 0.075 cm. Thus, the flame would be expected to penetrate the type I orange foam but not the type III red foam just as the experiments indicated (see Figure 11). At the 50 percent location, from Figure 18, D_h^* is 0.092 cm. This would indicate that the type I orange foam would also burn through at 50 percent but the data of Figure 11 indicate that it did not.

An empirical fit was made to the pressure drop data by using the information in the Scott circular (form 3645-R-0375) with the following result.

$$f = 5.352\ P_{pi}^{0.8481} \left(\frac{\rho v}{\mu}\right)^{-.15} \tag{55}$$

The values of the constants were determined using average values of f at 20 and 45 pores per inch. Solving for P_{pi} in terms of f_{COR} (i.e., $\rho v/\mu = 59021$ per ft) yields

$$P_{pi} = 0.9657\ f_{COR}^{1.179} \tag{56}$$

Table 2 shows calculated values of P_{pi} from Equation (56) for a number of foam samples that were cut from different locations in the bun. The nominal values of the pores per inch for each sample are also shown in Table 2. The agreement is reasonable from 15 to 45 pores per inch. Thus, pressure drop data can be used to determine the value of f_{COR} which can be used to determine the hydraulic diameter. If Equation (56) and (54) are combined, the result is

$$D_h = 0.4322\ f_{COR}^{-1.372} \tag{57}$$

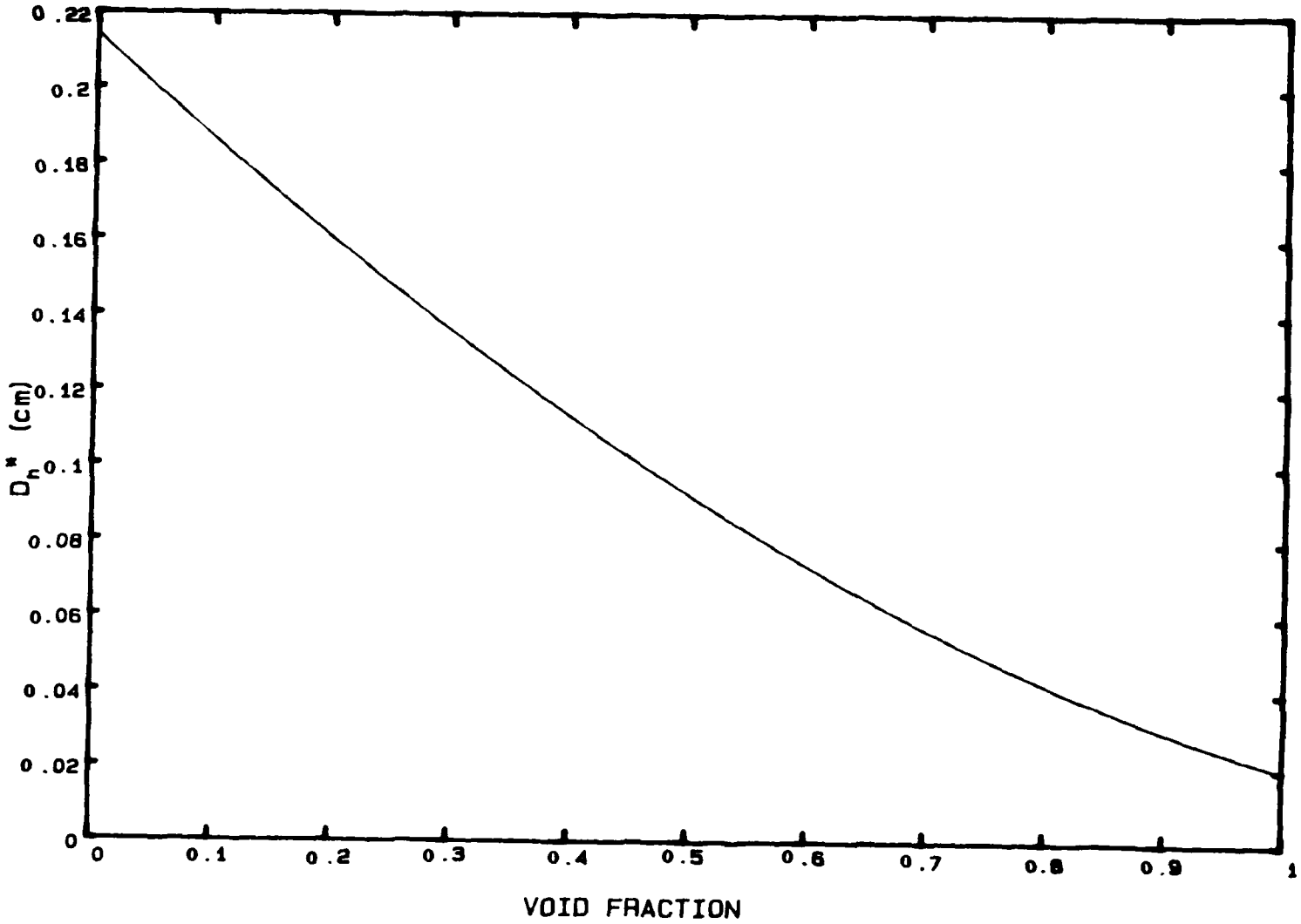

Figure 18. Critical value of the hydraulic diameter for propane versus flame position in the flame tube.

TABLE 2

CALCULATED PORES PER INCH COMPARED TO THE NOMINAL VALUE FOR VARIOUS FOAM SAMPLES

FOAM ID	NOMINAL PORES PER INCH	f_{COR}	CALCULATED PORES PER INCH
T15-FV	15	10.20	14.9
-REV		10.01	14.6
-RV		12.17	18.4
-LV		9.36	13.5
-BH		8.15	11.5
-MH		.07	13.0
-TH	15	9.47	13.7
T4-A1M1	15	8.08	11.5
-A1M2		8.50	12.2
-B2M1		8.26	11.8
-B2M2		8.45	12.1
-C3M1		8.23	11.7
-C3M2	15	8.62	12.4
T20-RV	20	13.63	21.0
-LV		15.93	25.3
-BH		9.25	13.3
-DB		14.08	22.0
-MH		11.54	17.0
-TH		11.73	18.0
-REV	20	15.32	24.0
T3-A1M1	25	15.02	24.0
-A1M2		14.84	23.7
-C2M1		14.69	23.4
-C2M2		14.63	23.3
-E3M1		14.08	22.2
-E3M2	25	13.85	21.8
T5-A1M1	25	16.17	26.2
-A1M2		15.30	24.5
-B2M1		14.37	22.8
-B2M2		15.28	24.5
-C3M1		16.03	25.9
-C3M2	25	16.08	26.0
W742-V1-9	45	24.73	42.4

The value of D_h calculated from Equation (57) can be compared to D_h^* determined with Figure 18 to estimate at what void fraction the foam would no longer extinguish the flame. For the cases when the foam does not extinguish the flame, the value of D_h, calculated from Equation (57), can be used with the equations from the heat loss studies to determine the effect on the final value of the overpressure.

RESULTS AND RECOMMENDATIONS

A number of useful results were obtained during this research effort:

- A correlation was made between the number of pores per inch and hydraulic diameter of the foam.
- A correlation was made between the friction coefficient f_{COR} and the number of pores per inch of the foam.
- A generalized flame quenching criteria was presented.
- The variation of the critical hydraulic diameter with pressure and temperature was presented.
- A procedure for relating the critical hydraulic diameter to the flame position in the flame tube was developed.
- The void fraction required to produce burn through the foam was determined.
- An empirical equation was developed for the cooling phase in the flame tube.
- A theory, that compared favorably to experiments, for predicting flame tube overpressure was developed.
- It was shown that the flame arrestor results are independent of f_{COR} (or pore size) and thickness provided it quenches the flame.
- Pressure waves are transmitted through the foam with little or no attenuation.

- A pressure rise theory was developed.
- The equations and procedures presented enable the performance of the flame tube to be determined from the values of the initial temperature, initial pressure, void fraction, and hydraulic diameter of the foam.

It is recommended that the known variation of the flame speed and adiabatic flame temperature be integrated into the theory. Also, the theory should be extended to determine the overpressure that results when the flame continues to burn through the foam.

REFERENCES

1. Maurice O. Lawson and John E. Minardi, "Study of Aero Propulsion Laboratory Pressure Drop Rig and Recommended Test Procedure," UDR-TR-84-139, University of Dayton Research Institute, Dayton, Ohio, December 1984.

2. J. E. Minardi and M. O. Lawson, "Summary Report on Crest-Foam Qualification Tests," UDR-TR-85-87, University of Dayton Research Institute, Dayton, Ohio, July 1985.

3. Joseph M. Kuchta, Ralph J. Cato, and Whittner H. Gilbert, "Flame Arrestor Mateirals for Fuel Tank Explosion Protection," AFAPL-TR-70-40, Air Force Aero Propulsion Laboratory, Wright-Patterson Air Force Base, Ohio, July 1970.

4. Kenneth K. Kuo, Principles of Combustion, John Wiley & Sons, Inc., New York, New York, 1986.

5. Thomas A. Hogan and Charles Pedriani, "Flame Tube and Ballistic Evaluation of Explosafe Aluminum Foil for Aircraft Fuel Tank Explosion Protection," AFWAL-TR-80-2031, Air Force Wright Aeronautical Laboratories, Wright-Patterson Air Force Base, Ohio, April 1980.

6. Terence Dixon, "Gross Voided Flame Arrestors for Fuel Tank Explosion Protection," AFAPL-TR-73-124, Air Force Aero Propulsion Laboratory, Wright-Patterson Air Force Base, Ohio, February 1974.

7. H. C. Hottel and R. B. Egbert, "Radiant Heat Transmission from Water Vapor," presented at the Joint Symposium with the Heat Transfer Division of the American Society of Mechanical Engineers at the Boston, Massachusetts, meeting, May 13, 1942. (Transactions, American Institute of Chemical Engineers, pp. 531-568.)

8. H. C. Hottel, "Heat Transmission by Radiation from Non-Luminous Gases," Transactions, American Institute of Chemical Engineers, Vol. 19, 1927, pp. 173-205.

9. Robert B. Egbert, "Heat Transmission by Radiation from Gases," Ph.D. Dissertation, Massachusetts Institute of Technology, 1942.

10. V. Ganapathy, Basic Programs for Steam Plant Engineers, Marcel Dekker, Inc., New York, New York, 1986.

11. R. P. Wilson, Jr. and S. Attalah, "Design Criteria for Flame Control Devices for Cargo Venting Systems," CG-D-157-75, U.S. Coast Guard, Department of Transportation, August 1975.

*U.S.Government Printing Office: 1987 — 748-061/61067

END

11-87

DTIC